Geo-information Science and Remote Sensing

Thesis Report GIRS-2017-27

EVALUATING THE POTENTIAL OF SENTINEL-2 AND LANDSAT IMAGE TIME SERIES FOR DETECTING SELECTIVE LOGGING IN THE AMAZON

Dainius Masiliūnas

October 11, 2017

WAGENINGEN
UNIVERSITY & RESEARCH

Evaluating the potential of Sentinel-2 and Landsat image time series for detecting selective logging in the Amazon

Dainius Masiliūnas

Registration number 93 04 07 546 120

Supervisors:

Dr Jan Verbesselt
Dr Marielos Peña-Claros

A thesis submitted in partial fulfilment of the degree of Master of Science
at Wageningen University and Research Centre,
The Netherlands.

October 11, 2017
Wageningen, The Netherlands

Thesis code number: GRS-80424
Thesis Report: GIRS-2017-27
Wageningen University and Research Centre
Laboratory of Geo-Information Science and Remote Sensing

Abstract

Logging in the Amazon is primarily selective, with individual commercial trees cut down, leaving the others untouched. The direct effects of selective logging are difficult to quantify using remote sensing techniques due to the small extent of treefall gaps left after logging, and the quick canopy regrowth that follows. In this thesis, the time series of five vegetation indices (NDVI, NDMI, NBR, EVI, MSAVI) derived from Landsat 7 ETM+, Landsat 8 OLI and Sentinel-2 MSI imagery were evaluated for detecting selective logging features in three study sites in the Amazon. Logging roads and log decks could be identified both manually and automatically using imagery from any of the sensors, given enough history for building a stable seasonal model. Skid trails could not be identified using any sensors. Treefall gaps could not be reliably identified using Landsat imagery, but 43% of treefall gaps in known treefall locations could be manually identified in Sentinel-2 MSI imagery. From the vegetation indices, NDMI was the most sensitive to reflectance changes in treefall gaps after logging, followed by NBR, due to their sensitivity to changes in forest internal shadowing. NDVI was sensitive only to soil and non-photosynthetic vegetation uncovered after logging. Changes in EVI and MSAVI reflected changes in both internal shadows and uncovered soil and non-photosynthetic vegetation, but the magnitude of change was the lowest of all indices tested. This study shows that it is possible to detect treefall gaps in Sentinel-2 imagery, and potentially automate it in the future, so that estimates of selective logging volumes could be based on direct observations of treefall gaps, rather than assuming a correlation between roads or log decks and the volume of timber harvested.

Keywords: selective logging, treefall gap, logging road, skid trail, log deck, time series, Landsat, Sentinel-2, BFAST, Amazon, Peru, Guyana

Contents

1 Introduction

Selective logging is a process by which particular commercial species of trees in a forest are cut down for timber production according to criteria such as size and species. This type of logging has become common practice in tropical forest areas, where high biodiversity leads to a highly complex forest structure with trees of different sizes, shapes and properties. Commercial trees tend to be spread over an area, mixed with trees of lower commercial value. Once a large tree is cut down, it is likely to fall on neighbouring trees. This causes a disturbance in the area, especially if only the tree stem is extracted, leaving the canopy (large branches and foliage) on top of the understory and forest floor. This disturbance can be visible from above in the form of logging gaps, with a crown zone where the top of the tree canopy had fallen, and trunk zone where the trunk had fallen, arranged in an elliptical pattern from the tree stump.

Selectively logged forests most often remain forests after the logging event (Asner et al., 2006), but they are disturbed, as wood from large trees is removed from the ecosystem, causing forest degradation. Succession is initiated at the points of disturbance, resulting in the replacement of mature, climax community trees with young pioneer species. Selective logging may be done illegally (Rutishauser et al., 2015), in which case the result is loss of biodiversity and lowered forest resilience. However, it could also be part of sustainable forestry practices, in which case trees are selected and logged in a way that reduces this negative impact to the forest and creates favourable conditions for succession in managed forests (West et al., 2014; Keller et al., 2004). This practice is called **R**educed-**I**mpact **L**ogging (RIL). Selective tree dieoff may also be caused by natural events, such as windstorms and landslides (Frolking et al., 2009).

Even though selective logging is widespread in tropical forests, little is known about the real scale of logging activities. Selective logging is difficult and expensive to detect and quantify due to the remoteness of the affected forests, problematic accessibility, and the disappearance of logging traces over time due to regrowth. While remote sensing approaches have been employed for detecting selective logging in the past (Shimizu et al., 2017; Frolking et al., 2009; Broadbent et al., 2006; Keller et al., 2004), their success has been limited. A typical current-day selective logging operation leaves four types of traces that are potentially detectable using remote sensing: logging roads, which are built for easier transportation of logs to sawmills by lorries; log decks, which are clearings in which logs are stored until they can be picked up by the lorries; skid trails, which are made by skidders in order to gain access to the location of the felled tree and drag the logs to the log decks; and treefall gaps, which are formed in the forest canopy when a tree is cut down (Asner et al., 2002). The two former logging features are rather distinct and have been successfully detected from satellite imagery, however, their prevalence is not necessarily a direct indication of the magnitude of the performed selective logging activities. In some selective logging campaigns, depending on the logging intensity and distance to major roads, only minor roads are made and log decks are omitted entirely; skidders can carry logs one by one to the nearest existing road, rather than mandating the creation of new roads and log decks (Read, 2003). Thus treefall gaps and skid trails are the most direct evidence of selective logging intensity. In comparison to all of the other logging features, treefall gaps are by far the most spatially extensive (Asner et al., 2002).

The detection of treefall gaps and skid trails from optical satellite imagery so far has been challenging. While there are some cases in which the treefall gaps have reportedly been detectable (Frolking

et al., 2009), either very high resolution, long revisit time sensors were needed (Read, 2003), or the differences in reflectance compared to unlogged forest were found to be minimal (Asner et al., 2004; Broadbent et al., 2006). With the advent of new satellites and sensors, such as Landsat 8 and Sentinel-2, the ability to detect such small variations in the canopy should improve due to higher spatial resolutions and more frequent revisit times. In the tropical regions, the revisit time is particularly important due to frequent cloud cover, especially during the rainy season, which may inhibit monitoring selective logging sites shortly after the logging event has happened.

If it is doable to detect and track individual treefall gaps in time, it would also allow for estimating the length of succession in the particular area. While full secondary forest regrowth after logging may take up to 125 years (Rutishauser et al., 2016), the canopy closure at the selective logging site happens much faster, estimated at 3-6 months depending on the size of the disturbance and the chosen definition of recovery (Broadbent et al., 2006). Precise knowledge on selective logging event frequency, their intensity and the recovery time after selective logging is important for the countries in the area for setting logging policies, and as a contributor to forest degradation forms a key part of the United Nations **R**educing **E**missions from **D**eforestation and forest **D**egradation (REDD+) programme. It is also important to monitor such activity in order to minimise illegal logging and allow for more precise estimation of existing and historical carbon stocks (Piponiot et al., 2016; Pinard and Cropper, 2000), as well as for climate change modelling (Rutishauser et al., 2015). However, so far such estimation has been challenging (Piponiot et al., 2016) and thus it has only been performed based on chronosequences, which are forest plots of different timespan since logging (Broadbent et al., 2006), or extrapolated from recovery rates (Rutishauser et al., 2015). Making use of the full archive of satellite imagery to construct a time series could potentially allow for a more precise estimate of regrowth time as well as per-tree statistics, while eliminating bias which may otherwise arise due to the different locations and logging times of the investigated plots. In the long run, a system could be developed that detects such selective logging events and provides for both near-real-time monitoring of selective logging events and information on whether and when selective logging has occurred in the past. This would in turn enhance the knowledge on the current and past state of tropical forests, provide information on how widespread selective logging is and help quantify its effects on the tropical forest ecosystem. In addition, knowing the location of disturbances and their canopy recovery times would allow for a more accurate large-scale estimation and monitoring of biomass and carbon stocks in tropical forests by enhancing tropical forest post-logging regrowth models (Herault et al., 2010).

2 Problem definition and research questions

While satellite image time series trajectory analysis has been relatively well-established in the recent years, few studies focus on the detection of small-extent selective logging features (skid trails and treefall gaps) using this technique. Most studies of tropical forest regrowth make use of chronosequences of plots with different age instead. However, time series analysis is well-suited for this purpose, because it allows detecting the disturbance time and regeneration length in a much more precise manner. In addition, time series analysis is not affected by site-specific effects, as is the case with chronosequences.

Another advantage of using satellite imagery for detecting selective logging is that it is spatially exhaustive. Satellites constantly monitor surface reflectance over the entire globe, it is not limited to a select number of test plots. With the advent of the Sentinel-2 programme, the public now has access to data that is of much finer spatial resolution (10×10 m, as opposed to 30×30 m of Landsat) while maintaining a short revisit time. This new data may allow better detection and monitoring of selective logging sites, including treefall gaps and skid trails, compared to what was possible before.

The goal of this thesis is to evaluate the potential and added value of new satellite imagery for detecting selective logging events by employing time series detection methods on Sentinel-2 and Landsat 8 imagery in three areas in the Amazon region where known selective logging has occurred. The research questions that the thesis aims to answer are:

1. How well can selective logging events be detected by employing time series methods on optical satellite imagery?

2. What is the sensitivity of different vegetation indices for detecting selective logging treefall gaps?

3 Data and methods

To assess the detectability of selective logging events, three areas of interest were selected in the Amazon rainforest where selective logging is known to have taken place. Five vegetation indices derived from Landsat 7, Landsat 8 and Sentinel-2 imagery were used to construct time series in order to test detection of selective logging features, especially treefall gaps. High resolution imagery from the **A**dvanced **S**paceborne **T**hermal **E**mission and Reflection **R**adiometer (ASTER) programme and very high resolution imagery from DigitalGlobe satellites were used for validation.

3.1 Sensor characteristics

3.1.1 Landsat 7 ETM+ and Landsat 8 OLI

Data from two Landsat missions was used to obtain long-term dense time series of ground observations at 30 m resolution. Landsat 7, launched in 1999, carries the **E**nhanced **T**hematic **M**apper **Plus** (ETM+) instrument that captures imagery in 3 visible light bands, one **N**ear **I**nfra**r**ed (NIR) band, two **S**hort**w**ave **I**nfra**r**ed (SWIR) bands, one thermal band and one broadband panchromatic band (U.S. Geological Survey, 2017a). Landsat 8, launched in 2013, carries the **O**perational **L**and **I**mager (OLI) instrument that captures imagery in comparable bands to ETM+, but also adds an additional thermal band as well as coastal aerosol and cirrus bands (U.S. Geological Survey, 2017b). Both of the satellites have a revisit time (at the study sites) of around two weeks, and continue transmitting images to this day, although in 2003 Landsat 7 experienced a Scan Line Corrector failure that resulted in it transmitting 22% less data than before. The Landsat collection data is available from the **U**.**S**. **G**eological **S**urvey (USGS) Earth Resources Observation and Science (**E**ROS) Center **S**cience **P**rocessing **A**rchitecture (ESPA) system preprocessed into ground reflectance (Level 2A), as well as vegetation indices derived from the reflectance products. The products are in the **U**niversal **T**ransverse **M**ercator (UTM) coordinate system.

3.1.2 Sentinel-2 MSI

Sentinel-2 is a satellite launched in 2016 by the **E**uropean **S**pace **A**gency (ESA) that carries the **M**ulti-**s**pectral **I**mager (MSI) instrument, which captures 12 optical bands at varying spatial resolutions: the three visible bands and the NIR band are available in 10 m resolution; the two SWIR, three red edge bands and narrow-band NIR in 20 m resolution; and coastal aerosol, cirrus and water vapour bands at 60 m resolution (SUHET, 2015). The Sentinel-2 products are available from the ESA Sentinel Data Hub at the Level 1C processing level (top-of-atmosphere radiance). Due to how recent the satellite is, its imagery was only used for the Guyana 2017 field campaign area (see section 3.3). The logging gaps from the 2013 and 2014 selective logging sites would be indistinguishable from the surroundings by 2016.

3.1.3 ASTER and DigitalGlobe

ASTER is a joint NASA-Japan government mission and an instrument (comprised of three separate sensors) on board the Terra satellite, launched in 1999, which captures images in 14 spectral bands with varying resolutions: 15 m for the two visible bands (green-yellow and red) and two NIR bands (nadir and backwards-facing), 30 m for six SWIR bands and 90 m for five thermal bands. The revisit time for the images taken during the day varies from 0 to 11 times per year. Since 2016, the data is freely available through the USGS Land Processes Distributed Active Archive Center as Level 2 (surface reflectance) products (NASA LP DAAC, 2006). On April 6, 2008 the SWIR sensor overheated, resulting in completely saturated and thus unusable SWIR bands from that date up to the present (Meyer et al., 2015).

Images from the DigitalGlobe satellite fleet (GeoEye-1, WorldView-2), available through Google Earth, were also used for validation. These images are displayed in red, green and blue visible bands and have a pan-sharpened spatial resolution of 0.5 m. The revisit time in the areas of interest vary but is very long (several years per visit).

3.2 Vegetation indices

Five vegetation indices, as defined by U.S. Geological Survey (2017c), were compared in this study and are described in the following subsections. **S**oil **A**djusted **V**egetation **I**ndex (SAVI) and Normalised Burn Ratio 2 were not used due to their similarity with **M**odified **S**oil **A**djusted **V**egetation **I**ndex (MSAVI) and **N**ormalised **B**urn **R**atio (NBR), respectively. In the case of Landsat imagery, precomputed vegetation indices were used, and for the other imagery, vegetation indices were derived from the imagery manually.

3.2.1 NDVI

Normalised **D**ifference **V**egetation **I**ndex (NDVI) is a commonly used vegetation index that is a ratio between the red and NIR bands:

$$NDVI = \frac{\rho_{NIR} - \rho_{Red}}{\rho_{NIR} + \rho_{Red}}$$

where ρ_{NIR} is the surface reflectance in the spectral band centred around 830 nm and ρ_{Red} is the surface reflectance in the spectral band centred around 660 nm (Tucker et al., 1979).

NDVI is easy to interpret and has a range of 0-1, but it is known to be insensitive to small changes in areas with dense vegetation, as the vegetation index saturates (Huete et al., 1999). In addition, cloud shadows over vegetation have NDVI values close to 1, because the values of the red band are close or equal to zero.

3.2.2 EVI and MSAVI

In order to overcome the shortcomings of NDVI, two more complex vegetation indices have been developed: **E**nhaced **V**egetation **I**ndex (EVI) and the SAVI family. EVI is designed to not saturate with high biomass the way NDVI does, and reduce atmospheric and background noise (for instance, thin clouds are compensated for). It requires the use of the blue visible band and several coefficients, and in this study the default ones adopted by NASA were used:

$$EVI = 2.5 \cdot \frac{\rho_{NIR} - \rho_{Red}}{\rho_{NIR} + 6 \cdot \rho_{Red} - 7.5 \cdot \rho_{Blue} + 1}$$

Study site	Logging date	Known logged trees	Landsat 7 ETM+		Landsat 8 OLI		Sentinel-2 MSI	
			Obser-vations	Stable history	Obser-vations	Stable history	Obser-vations	Stable history
Peru	2013-11	9	731	Yes	180	No	0	No
Guyana 2014	2014-11	9	335	Yes	93	No	0	No
Guyana 2017	2017-01	16	672	Yes	186	Yes	70	No

Table 3.1: Summary of satellite imagery used for each study site. Observations are the total number of images processed for the study site, stable history indicates whether there were enough observations before the logging event to allow for analysis based on time series.

Here, ρ_{Blue} is the surface reflectance in the blue band (centred around 485 nm in ETM+) (Huete et al., 1999). Cloud shadows have a low EVI value, as opposed to NDVI.

The SAVI family was developed for solving the issue of vegetation on different soil backgrounds having an effect on NDVI. MSAVI is a modification of SAVI to maximise the reduction in soil background effects and increase the dynamic range of the vegetation signal (Qi et al., 1994). In this case the coeffiecients employed by NASA were used as well:

$$MSAVI = \frac{2 \cdot \rho_{NIR} + 1 - \sqrt{(2 \cdot \rho_{NIR} + 1)^2 - 8 \cdot (\rho_{NIR} - \rho_{Red})}}{2}$$

In the study area, MSAVI visually appears very similar to EVI, the main apparent difference is the lack of atmospheric noise reduction in MSAVI. However, MSAVI does not require the blue band, which allows calculation of MSAVI with the ASTER sensor that does not capture the blue band.

3.2.3 NDMI and NBR

Normalised **D**ifference **M**oisture **I**ndex (NDMI) and NBR are vegetation indices that are a normalised ratio between reflectance in the blue band and the SWIR band (Key et al., 2002). The difference is the wavelength of the SWIR band:

$$NDMI = \frac{\rho_{NIR} - \rho_{1600}}{\rho_{NIR} + \rho_{1600}}$$

$$NBR = \frac{\rho_{NIR} - \rho_{2220}}{\rho_{NIR} + \rho_{2220}}$$

ρ_{1600} indicates surface reflectance in the SWIR band centered around 1600 nm, whereas ρ_{2220} indicates surface reflectance in the SWIR band centered around 2220 nm. These vegetation indices are related to moisture in that water interferes with reflectance in the SWIR region, and dry leaf biomass has a similar reflectance in NIR as in SWIR, whereas a healthy leaf has lower reflectance in SWIR (Cibula et al., 1992).

NBR is commonly used for selective logging detection, as it is perceived to be more sensitive to disturbance events (Schneibel et al., 2017; Shimizu et al., 2017). Both NBR and NDMI are insensitive to cloud shadows, since they appear to lower the reflectance in both NIR and SWIR equally.

3.3 Field campaigns

To be able to detect treefall gaps and other selective logging features, the exact location of trees that have been selectively logged and the time of logging was needed. For this purpose, the metadata of selective logging site lidar scans by Gonzalez de Tanago Menaca et al. (2017) was used. Data

about three areas of the Amazon during different years was used (see figure 3.1), where a team of researchers from **W**ageningen **U**niversity & **R**esearch (WUR) took lidar scans of a number of trees that had been selected to be logged. Not all of the trees that had been logged in the selective logging campaigns were scanned, and a number of scans were taken of trees that ended up not getting logged. In this study, only the metadata (site location information) of the lidar scans were used, not the lidar scan data itself. Satellite imagery of each of these areas was used in order to attempt detection of selective logging features, see table 3.1 for a summary.

3.3.1 Peru, 2013

The first field campaign was in November of 2013 in the Madre de Dios region, Peru. The selective logging operation took place in a forest east of the village Planchón, which is 37 km north of the region's capital city Puerto Maldonado. This region has a dry and a wet season, the latter spans from December to March. In the region, agricultural areas are encroaching upon previously intact forest (Scullion et al., 2014). Around Planchón, the agricultural fields are gradually expanding towards the forest from the Interoceanic Road that crosses Puerto Maldonado and goes through Planchón to Bolivia and Brazil.

The selective logging campaign was carried out by local villagers who obtained a permit for selective logging and harvesting of Brazil nuts (*Bertholletia excelsa* Humb. & Bonpl.) in a Brazil nut concession in a natural forest. The villagers did not have logging equipment such as skidders; instead, logs were processed on the spot using chainsaws, and the resulting planks were transported from the forest to the nearest road on tricycles. The larger trees in the study area have a canopy crown size of 20-30 m.

Ten trees to be cut down were scanned from 8 positions arranged in 30 by 50 m rectangles. The trees that were slated for logging were located on one end of the rectangle and were cut in a way so that they fall towards the middle of the plots. The location of each of the positions was determined using two separate Garmin **G**lobal **P**ositioning **S**ystem (GPS) devices (except for the first tree, therefore it was excluded, resulting in 9 known treefall locations). After logging, the same sites were scanned a second time. In this study, the centroid of all the measured points for each scanning site was used as a the approximate location of the treefall gaps. The scan dates both before and after logging were recorded. The actual logging event happened in between the two dates, which were between 2 and 6 days apart.

In addition to the logged tree data, there were also point locations of treefall gaps (seven in total) that were made prior to the time of the scanning campaign. These gaps are likely to have been the result of previously logged trees in the selective logging campaign (although there is a chance that some of them have been created in earlier selective logging campaigns). In the case of gaps, only the post-logging date was recorded. Therefore in total 16 points from the Peru campaign were analysed for changes in reflectance following a selective logging event.

The area in which selective logging was known to take place was covered by Landsat images of path 2, rows 68 and 69. 731 Landsat 7 ETM+ images and 179 Landsat 8 OLI images of this area were processed in this study.

3.3.2 Guyana, 2014

In both of the Guyana selective logging campaigns, logging was carried out using RIL conventions by the Guyana Forestry Commission, a governmental organisation responsible for supervising forest concessions as well as granting and renewing logging permits in them. Lidar scanning was done as a research partnership between it and WUR under the project *SilvaCarbon*. The scans in these study

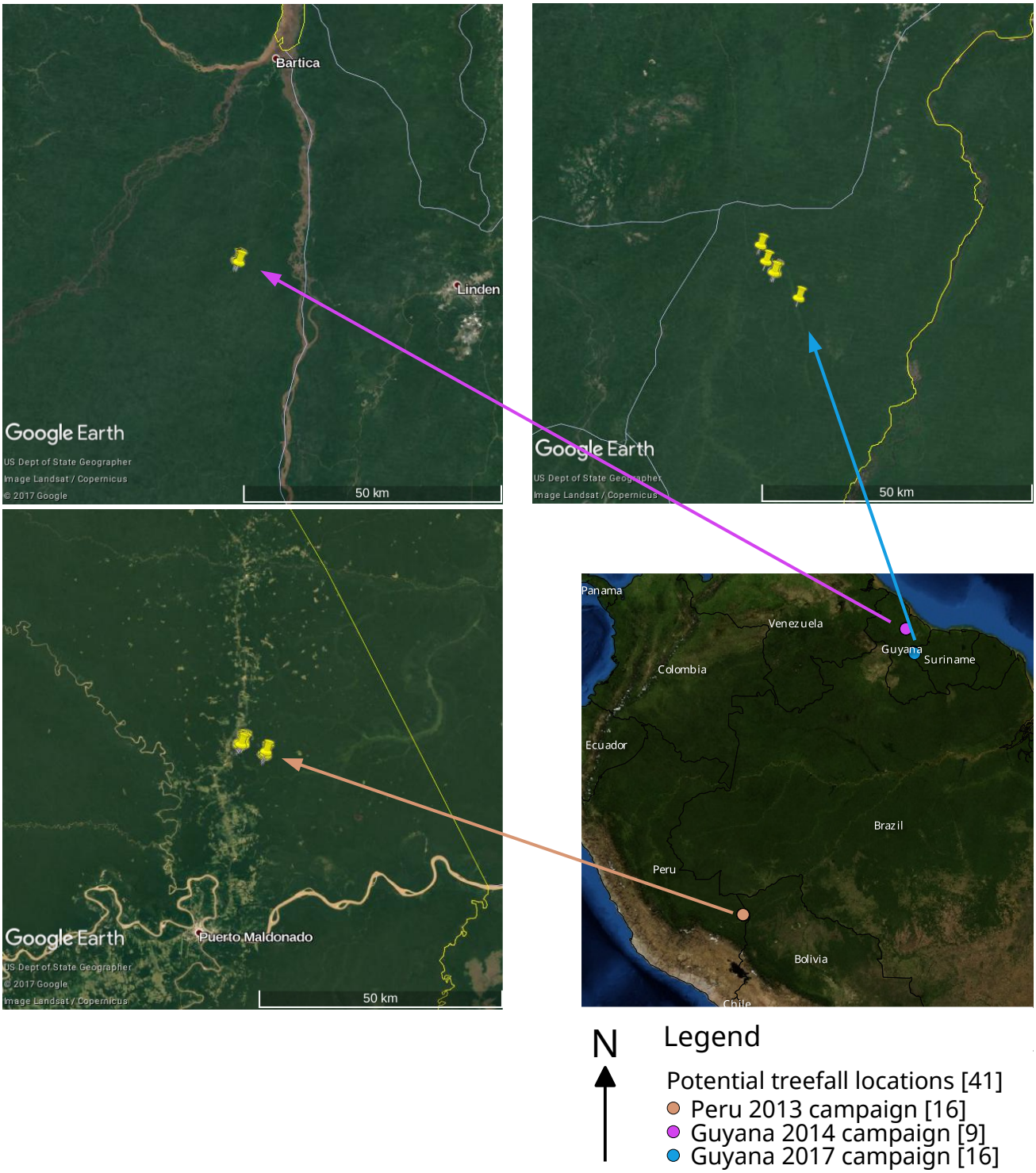

Figure 3.1: Study sites with potential locations and numbers of selective logging treefall gaps, in the context of South America.

sites were made by making plots of 30 by 40 m, and scanning from 13 positions. The trees were cut from a side towards the middle of the plot as well.

The second field campaign of those used in this study took place in the east of the Cuyuni-Mazaruni region of Guyana in November 2014. The nine selectively logged trees that were scanned in this area are located in the Wineperu concession of the Vairtana company, 40 kilometres south of the region's capital, Bartica. The town is connected to the selective logging sites by a road. The sites are very close to the road, 300 m away at most. Like the Peru campaign, the trees were scanned before and after the selective logging event. The area of selective logging was covered by Landsat images of path 231, row 56. In this study, 332 Landsat 7 ETM+ images of this area were processed in total.

3.3.3 Guyana, 2017

The third field campaign took place in the East Berbice-Corentyne region of Guyana in January 2017. The area where the trees were scanned is a very remote area at the end of a logging access road originally built in 1997 by the UNAMCO logging company, going south from the town of Kwakwani. After UNAMCO was closed in 2007, the road went unused until 2013, when the Ro-Anc company bought the concession and extended the road. For ease of timber extraction, a number of new primary logging roads (20 m across, gravel) were built in the logging site starting from 2014. Kwakwani is 85 kilometres north of the selective logging site.

In this campaign, a large number of inventoried trees were scanned, but trees were logged only in 16 of the locations. In some of these locations, clumps of more than one tree was inventoried and logged, with different heights and **D**iameter at **B**reast **H**eight (DBH), up to a total of 26 trees. The DBH class (20-40 cm, 40-60 cm, 60-80 cm, 80-100 cm and over 100 cm) of each tree was recorded. Some of the logged trees were relatively small (20-40 cm DBH) and below the canopy of larger trees. In addition, no post-logging scans were made, so it is unknown when exactly the logging events happened. In this study it was assumed that the logging happened a similar time after the pre-logging scan as in the previous campaigns.

The area of selective logging was covered by the Sentinel-2 granules 21NUE and 21NUF, and Landsat tiles with paths 230 and 231, row 57. 185 Landsat 8 OLI images and 70 Sentinel-2 MSI images of this area were processed in total.

3.4 Preprocessing workflow

Satellite imagery of all the products used were available either in the Level 1C (top-of-atmosphere radiance) or Level 2A (top-of-canopy reflectance) processing levels. For use with time series-based methods, this data had to be preprocessed further. All preprocessing past Level 2A data was done using the R programming language (version 3.3.1), and the produced scripts were made available online at <https://github.com/GreatEmerald/master-logging>. A flowchart of the process is shown in figure 3.2.

3.4.1 Top-of-canopy reflectance (Level 2A) processing

Sentinel-2 imagery is currently made available as Level 1C products. These products were processed into Level 2A products by using the `sen2cor` software, version 2.3.1 (Mueller-Wilm, 2016). `sen2cor` was set to use the 940 nm bands for water vapour correction, cirrus correction was enabled, a Digital Elevation Model from the Shuttle Radar Topography Mission was used for terrain correction and ozone column content data was set to be taken as best approximation from the metadata. All the other satellite imagery was already available in Level 2A and for those images this step was skipped.

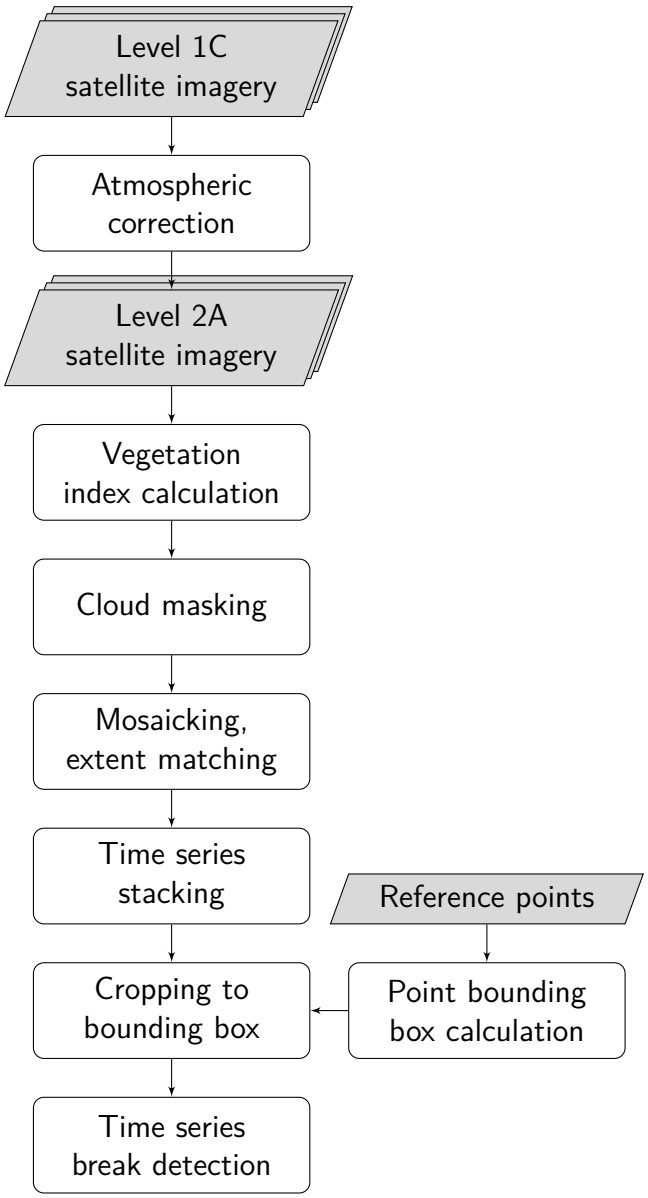

Figure 3.2: Satellite imagery preprocessing chain from imagery available for download into space-time cubes for time series analysis. Grey blocks are input and output data, rounded blocks are scripts that process the data.

3.4.2 Vegetation index calculation

For Sentinel-2 imagery, vegetation indices were calculated by using the formulae in section 3.2. In the case of NDMI and NBR, due to the lower spatial resolution of the SWIR bands (20 m vs 10 m), the SWIR bands had to be resampled to 10 m resolution by subdividing each pixel into four. Both nearest neighbour and bilinear interpolation resampling methods were tested.

For Landsat imagery, the vegetation indices were provided pre-calculated by ESPA, so this step was also skipped.

In the case of ASTER imagery, the post-2008 SWIR bands are oversaturated, and the blue band is not captured by the ASTER sensor, so only NDVI and MSAVI were calculated for this imagery.

3.4.3 Cloud masking

Clouds and cloud shadows had to be masked out from the satellite imagery to prevent spurious extremely high and low value observations in the time series. While some vegetation indices are insensitive to thin clouds and cloud shadows, all clouds and cloud shadows were masked in order to have consistent imagery for all vegetation indices in order to compare them. Masking involves replacing the reported reflectance values in clouded or shadowed areas of the images with **N**ot **A**vailable (NA) values.

For Landsat data, clouds detected using the `Fmask` algorithm (Zhu and Woodcock, 2012) and included in the pixel QA raster were masked out. Only pixels marked as clear (66 and 130 for ETM+, 322 for OLI) were kept, all other values were filtered out. This was done by using the R package `bfastSpatial`, development branch (Dutrieux and DeVries, 2014). In addition, values marked as oversaturated (reflectance values set to 20000) or fill (reflectance values set to -9999) in the reflectance images themselves were masked out as well.

For Sentinel-2 data, scene classification maps generated by `sen2cor` were used to mask out areas marked as no data, saturated, dark area, cloud shadows and all types of clouds.

3.4.4 Mosaicking

All of the study areas except for Guyana 2014 were located on the edge between two Landsat tiles or two Sentinel-2 granules. In order to make use of all the data available, tiles/granules from the same sensor taken at the same date were mosaicked together. Since the data that was mosaicked was in the form of vegetation indices, the rule applied when a pixel was covered by two images was to keep the higher pixel value of the two. This allows for filling in gaps left by masked out clouds and selecting the highest quality pixels. Since cloud shadows and clouds usually lower the value of vegetation indices, selecting higher values filters out the effects of clouds that were not detected (and thus not masked out in the cloud masking phase) and prevents negative outliers in the resulting time series.

In addition to mosaicking, in this step all tiles were padded with NA values in a way so that the extents of all images would match, in preparation for the time series stacking step.

3.4.5 Time series stacking

To make use of per-pixel vegetation index time series, all observations had to be stacked into one file with multiple layers, each layer representing one (potential) observation and containing information about the date of the observation. For Landsat data, this was done using the `bfastSpatial` package. For Sentinel-2 data, a script for stacking was created from scratch.

3.4.6 Cropping to treefall gaps

Tiles and granules cover a large area, whereas only the potential treefall gap areas were the focus of this study. Consequently, to minimise the area to search through, images were cropped to the area around the treefall gap reference points. First, reference points were transformed into the UTM projection that was used by the Landsat images of the area, then a buffer of 75 metre radius (150 metre diameter) was made around each point. Next, a bounding box of each buffer was calculated, and each time series stack was cropped to the bounding boxes. The result was one space-time cube per each reference treefall gap per each sensor. The spatial dimensions of the Landsat space-time cubes were 5 by 5 pixels, whereas Sentinel-2 spatial dimensions were 15 by 15 pixels.

3.4.7 Time series analysis

Lastly, pixels of the space-time cubes were analysed one by one by using the `BFAST` package which implements the **B**reaks **F**or **A**dditive **S**eason and **T**rend (BFAST) algorithm (Verbesselt et al., 2010) to attempt detection of selective logging features. This is done by using trajectory analysis: a seasonal model is fit to the data by making use of known stable history prior to a logging event. Then, deviations from the values predicted by the model (residuals) are analysed at the time when a selective logging event potentially could have taken place. If the magnitude of observations exceeds a certain threshold, the first such observation is marked as a detected change.

In addition to treefall gaps, some nearby logging features such as logging roads and shifting cultivation were analysed with BFAST as well. The individual layers of the space-time cubes were also analysed visually, also in larger context and with comparison with higher resolution imagery from ASTER, PlanetScope and DigitalGlobe imagery.

For Sentinel-2 MSI imagery analysis, BFAST could not be used due to the lack of stable history to train the seasonal model on. The Sentinel-2A satellite started transmitting imagery in October of 2015; and due to frequent cloud cover over the Amazon the image time series is sparse, with too few observations to determine the natural variance of the vegetation indices. Instead, for this imagery, the pixels of the known treefall location space-time cubes were inspected for visible changes in the area. Pixels that showed changes in NDVI (44 in total) and NDMI (36 in total) in at least two images following the logging event and stood out from the surrounding area were selected, and Welch's two-sample t-test was used to determine whether the differences in the vegetation index values before and after logging are significant, as well as to compare the estimated true means of each vegetation index before and after logging. For control purposes, the same tests were applied to four pixels furthest away from the centre of each reference point, while still being in the space-time cube of each known logged tree (106 m to the north-west, north-east, south-east and south-west from the centre), with the assumption that no selective logging occurred that far away from each reference point. Next, regressions were done between the area of each detected treefall gap and the DBH of the largest tree logged at the associated reference point. The largest tree was chosen because in several locations, clumps of trees of varying sizes were cut at once, and the smaller trees would be felled in the direction of the gap created by the largest tree. Finally, Pearson's correlation between all of the tested vegetation indices was calculated within the extent of the space-time cubes around the treefall gaps.

4 Results

4.1 Logging feature detectability

4.1.1 Treefall gaps and skid trails

Sentinel-2

In the Guyana 2017 study area, which was the only study area that had Sentinel-2 coverage, no skid trails could be identified using Sentinel-2 MSI imagery. From the 16 reference points of known logged trees, 9 treefall gaps could be identified, but only 7 of them with confidence (see table 4.1). Two of the reference points were within a 6 m distance from one another, which made them not distinct from one another, and several more areas with potential treefall gaps overlapped (see figure 4.1). In the other cases where the gap was not visible, an existing gap, logging road or log deck was nearby. In the case there is an existing logging gap, according to RIL conventions the tree should be felled in the direction of the gap in order to minimise canopy damage.

Of the treefall gaps that were visible, on average the changes in vegetation indices after logging affected 5 pixels (500 m^2 area) in NDVI and 4 pixels (400 m^2 area) in NDMI. The correlations between the size of the affected areas and the DBH of the logged tree were not significant in both NDVI ($r^2 = 0.26$, $p = 0.13$) and NDMI ($r^2 = 0.19$, $p = 0.21$), see figure 4.2. Treefall gap sizes in NDVI were correlated with DBH inversely, whereas in NDMI they were correlated directly.

When comparing all vegetation index values before and after the selective logging event in the pixels where change was apparent, the values of each vegetation index tested were significantly ($p < 0.003$) lower after logging than before it (see table 4.2 and figure 4.3). In figure 4.4 is an example of how the NDMI and NDVI time series of a treefall gap pixel looks like, compared to a pixel not on a treefall gap.

Landsat

In Landsat imagery of the Guyana 2017 study area, only 3 gaps within the vicinity of the known logged trees could be identified, compared to 9 in Sentinel-2 MSI imagery. The rest of the gaps were not visible either due to cloud cover in Landsat scenes, or due to pixel border effects: gap centre going

Study site and year	Known logged trees	Logged trees with known logging date	Identified gaps (low confidence)	Identified gaps (high confidence)
Peru, 2013	16	9	1	0
Guyana, 2014	9	9	4	0
Guyana, 2017	16	0	9	7

Table 4.1: Summary of known logged tree locations and identified treefall gaps. Trees with known logging date are trees with records of dates both before and after logging (the others were missing either one of the two dates). High confidence for gap identification means that at least two vegetation indices indicated a change and the change was persistent at least in two subsequent images right after the logging date.

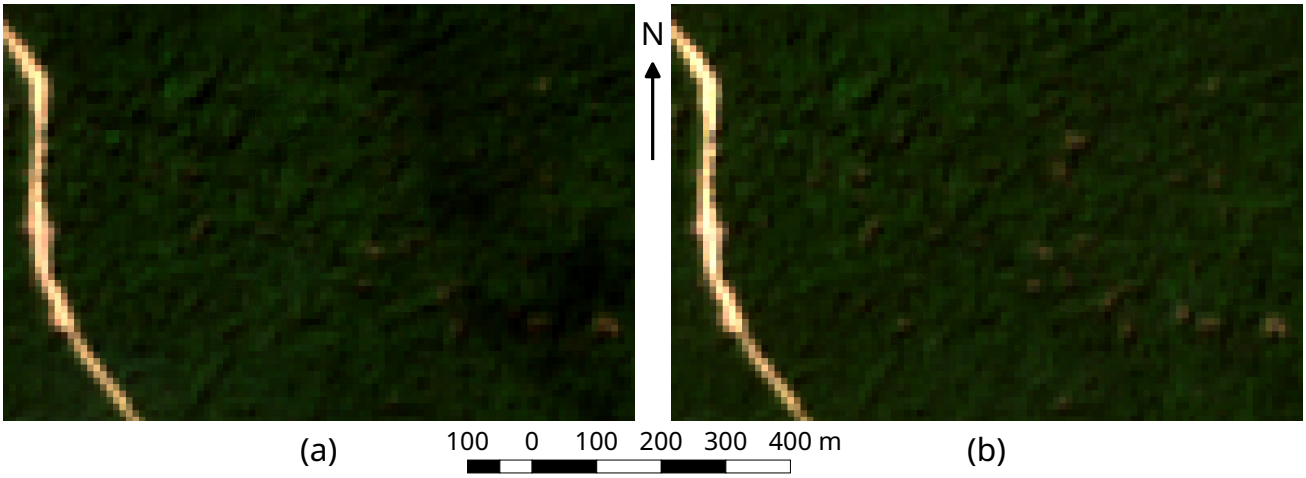

Figure 4.1: Sentinel-2 MSI true colour image subset from the Guyana 2017 study site. White circles indicate the 75 m radius around known logging locations. (a): site prior to known selective logging (January 13, 2017). The dark parts on the right are cloud shadows. (b): site after known selective logging (February 12, 2017).

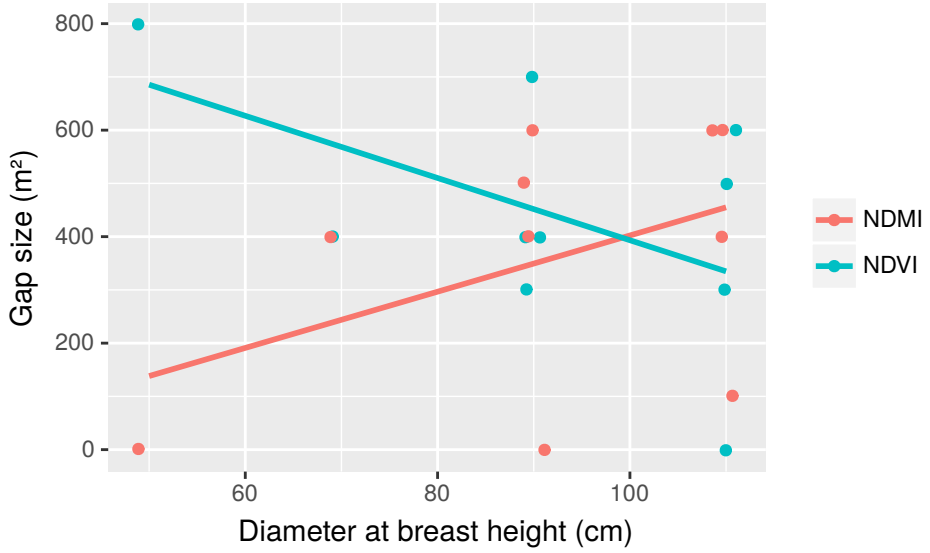

Figure 4.2: Regressions between the apparent gap size and the DBH of the largest tree logged at the location of each gap, grouped by vegetation index. The points are jittered to avoid overplotting. Precision of DBH is 20 cm, precision of gap size is 100 m^2, sample size is 10 gaps.

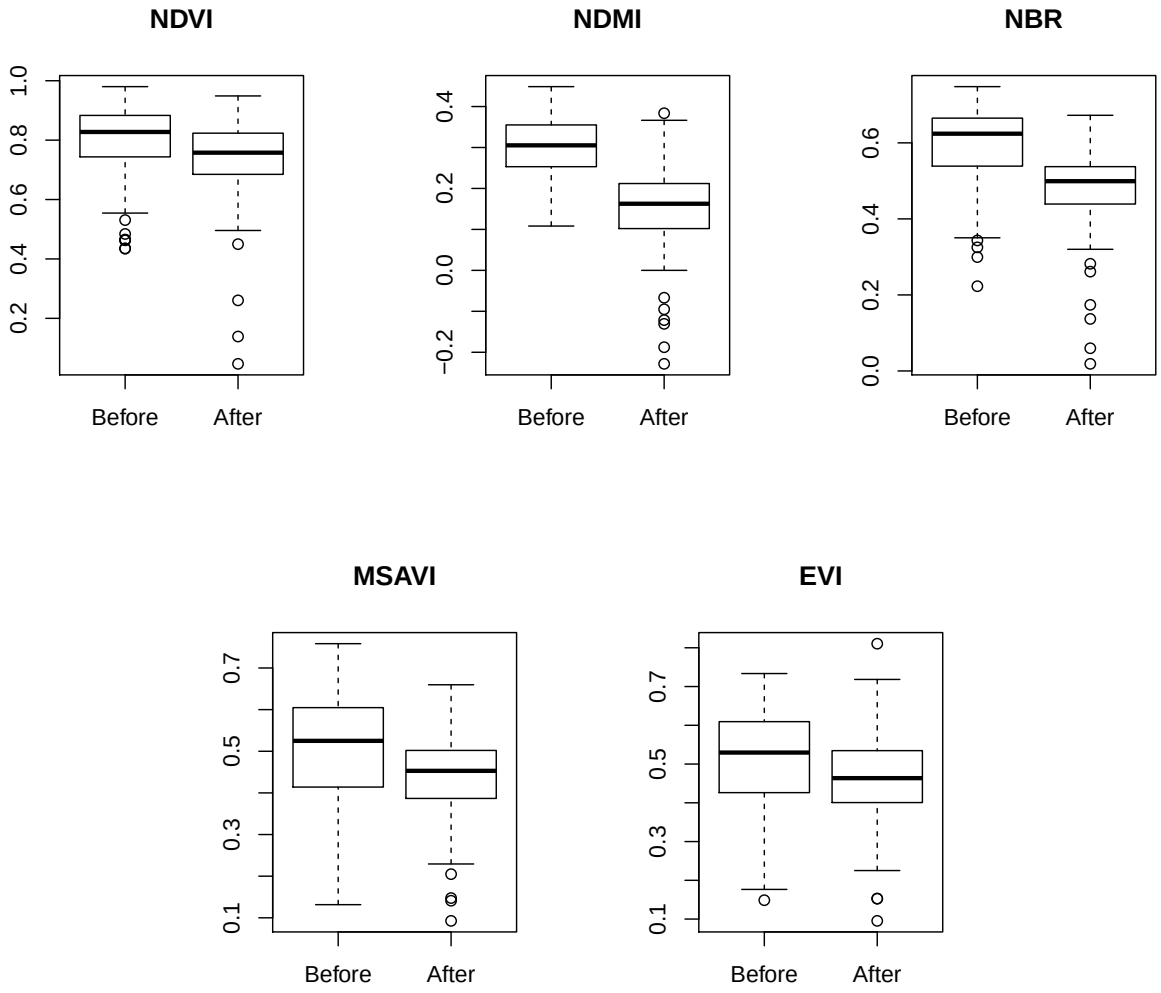

Figure 4.3: Distribution of vegetation index values before and after the known logging event in affected Sentinel-2 MSI pixels of the Guyana 2017 study site. The line in the middle of the box represents the median, the hinges of the box represent the 1st and 3rd quartiles, and the whiskers represent 1.5 of the interquartile range, circles are outliers.

Vegetation index	Mean before logging	Mean after logging	Change magnitude	p-value
NDVI in affected pixels	0.798±0.014	0.743±0.020	-0.055±0.024	<0.001
NDMI in affected pixels	0.300±0.010	0.150±0.017	-0.150±0.019	<0.001
NBR in affected pixels	0.599±0.012	0.481±0.017	-0.118±0.021	<0.001
MSAVI in affected pixels	0.494±0.020	0.438±0.017	-0.056±0.026	<0.001
EVI in affected pixels	0.504±0.019	0.463±0.019	-0.041±0.027	0.003
NDVI control	0.819±0.017	0.840±0.020	0.021±0.026	0.117
NDMI control	0.306±0.011	0.289±0.012	-0.018±0.016	0.036
NBR control	0.611±0.013	0.601±0.014	-0.009±0.019	0.338
MSAVI control	0.524±0.016	0.583±0.018	0.059±0.024	<0.001
EVI control	0.525±0.015	0.588±0.016	0.063±0.022	<0.001

Table 4.2: Change in vegetation index magnitude after a known logging event in the Guyana 2017 study area. Affected pixels are contiguous pixels with visually apparent change less than 75 m away from the location of known logged trees, control are four pixels 106 m away from each location of a known logged tree. Errors are 95% confidence intervals.

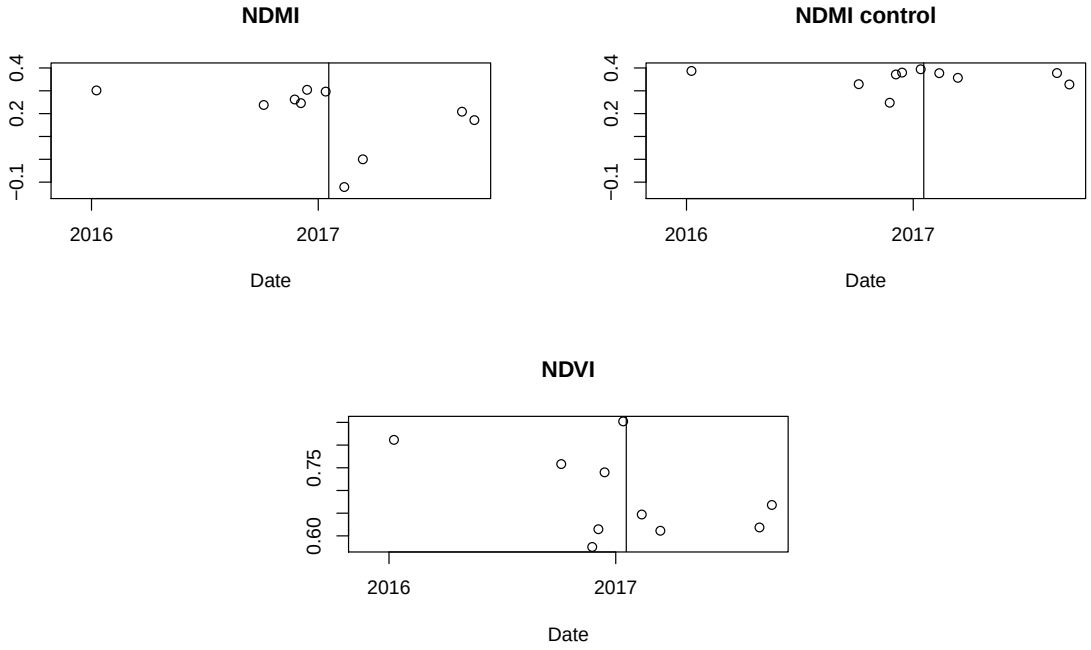

Figure 4.4: Time series of all Sentinel-2-derived NDMI and NDVI values for an example pixel where a treefall gap appeared, compared to a control pixel where no selective logging happened. The vertical lines indicate the date after which the selective logging event happened. The two low values in NDVI at the end of 2016 come from cloud shadows (NDMI compensates for them).

through the boundary of 2 or 4 pixels, therefore dispersing the signal into several pixels. That makes the treefall gaps unidentifiable due to a low signal-to-noise ratio. The gaps that can be identified in Landsat imagery also show a smaller magnitude of change due to the larger area covered by each pixel (900 m^2 compared to 100 m^2 in Sentinel-2 MSI).

BFAST analysis of Landsat imagery in the Guyana 2017 study site yielded only a single detection of a treefall gap, and only when using NDMI. The other two gaps, while visible when inspecting the time-space cube (the value of the pixel changes compared to the surroundings), are not detected by BFAST due to the low magnitude of change (see figure 4.5).

No treefall gaps could be detected using BFAST in other study sites. In the case of Landsat 8 OLI imagery of the Guyana 2014 site, a lot of false positives were generated due to too few observations in stable history (which was a period of less than one year, not enough to determine the natural variability). When using Landsat 7 ETM+ imagery of the same areas, no breaks were detected.

Skid trails were not visible from any of the satellite imagery used, in any of the study sites. In RIL, skid trails are planned in advance in a way that minimises the damage done, which means that there are no changes to the top of canopy that would be visible from satellite imagery.

ASTER

ASTER imagery of all the study sites were useful for better visualisation of the forest structure and the effects of forest features to vegetation index values, due to the finer pixel size compared to Landsat. However, the combination of a long revisit time and frequent cloud cover resulted in only one or two usable images per year, which is not enough for time-series-based analysis nor for statistical analysis. A comparison of images taken before and after the logging events (over a year apart) showed no outstanding differences. At 15 m resolution, individual trees cannot be visually picked out unless they stand apart from other trees or have a different seasonal cycle compared to neighbouring trees.

Another limiting factor of ASTER imagery is the range of digital numbers. Whereas Landsat and Sentinel-2 use the range of 0-10000 for digital numbers of each band, ASTER uses the range of 0-1000. This affects the range of derived vegetation index values: the smallest step between two values is 0.005. Any value in between is clamped to one or the other side and may not be distinguishable from the surroundings if neighbouring trees have similar values, which happens at the higher end of vegetation index saturation.

4.1.2 Clearcut areas, logging roads and log decks

Larger-scale disturbances associated with selective logging, such as main logging roads as well as clearcuts or slash-and-burn activities, were detectable from both Landsat and Sentinel-2 imagery. Given sufficient historical data, BFAST could be used to automatically detect such disturbances and determine the approximate time at which they happened, using any of the tested vegetation indices (see figures 4.6 and 4.7).

While the detection of such disturbances was possible, the presence of these disturbances varied greatly across the different study sites: in Peru and Guyana 2014, the selective logging campaigns were carried out close to an existing road, therefore no additional disturbances that would indicate that selective logging had occurred appeared in that area. In Guyana 2017, logging roads and log decks were built specifically for facilitating the selective logging campaign, some of them several years in advance (see figure 4.6). The Peru study site was the only one where land use was being changed from forest to shifting cultivation or rangelands, next to the selective logging site. The Landsat time series in that area was unique, with multiple points of disturbance spaced out over several years (see figure 4.7, top). The NDVI values after a clearcut go down quickly, and take a year to recover to

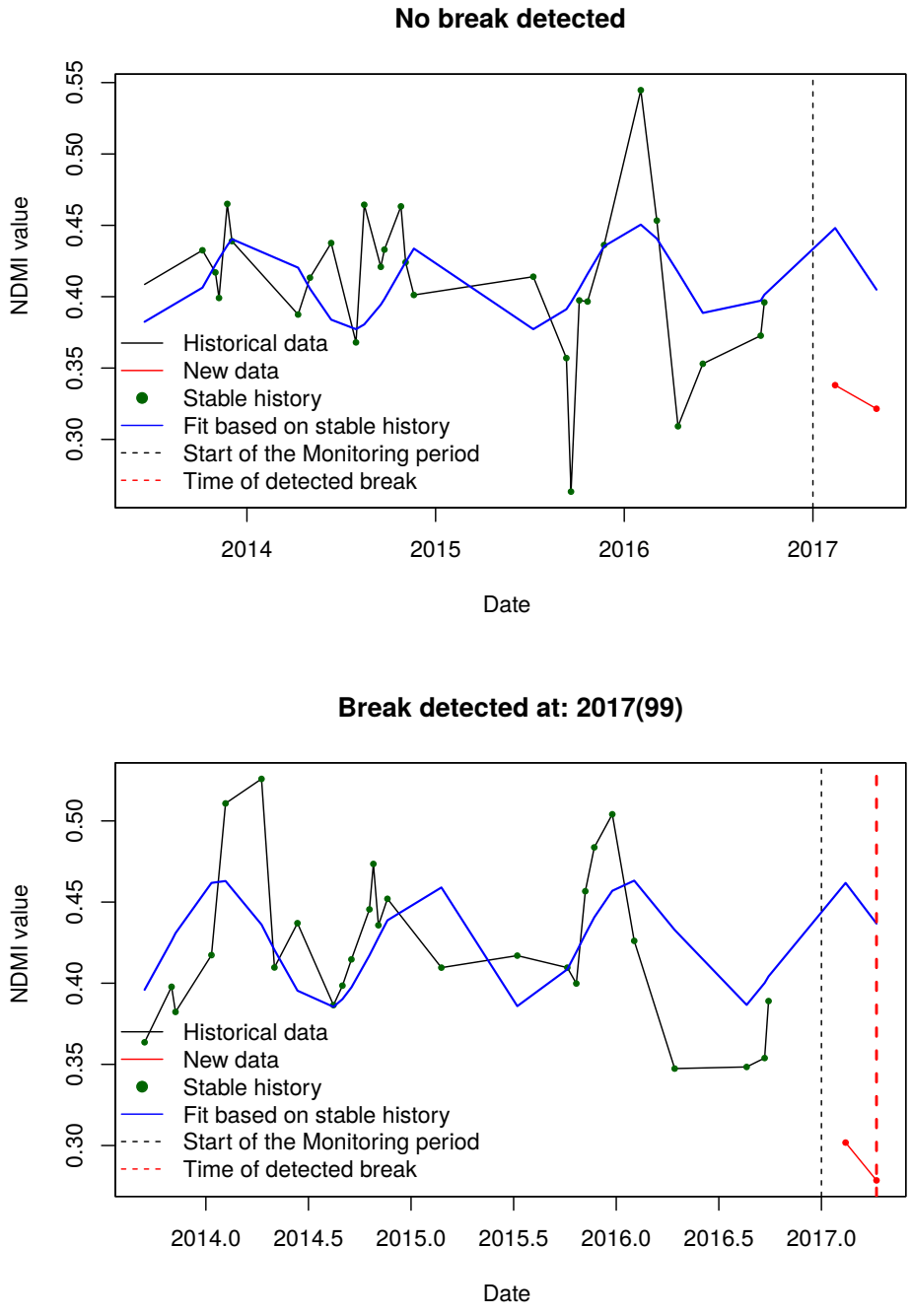

Figure 4.5: BFAST Monitor analysis of an NDMI time series for two Landsat 8 OLI pixels where treefall gaps are visible in Sentinel-2 MSI imagery of the same areas. Top: no change is detected due to too low magnitude of change, and some unfiltered clouded pixels in the history period. Bottom: change is detected successfully, as indicated by the red dashed line.

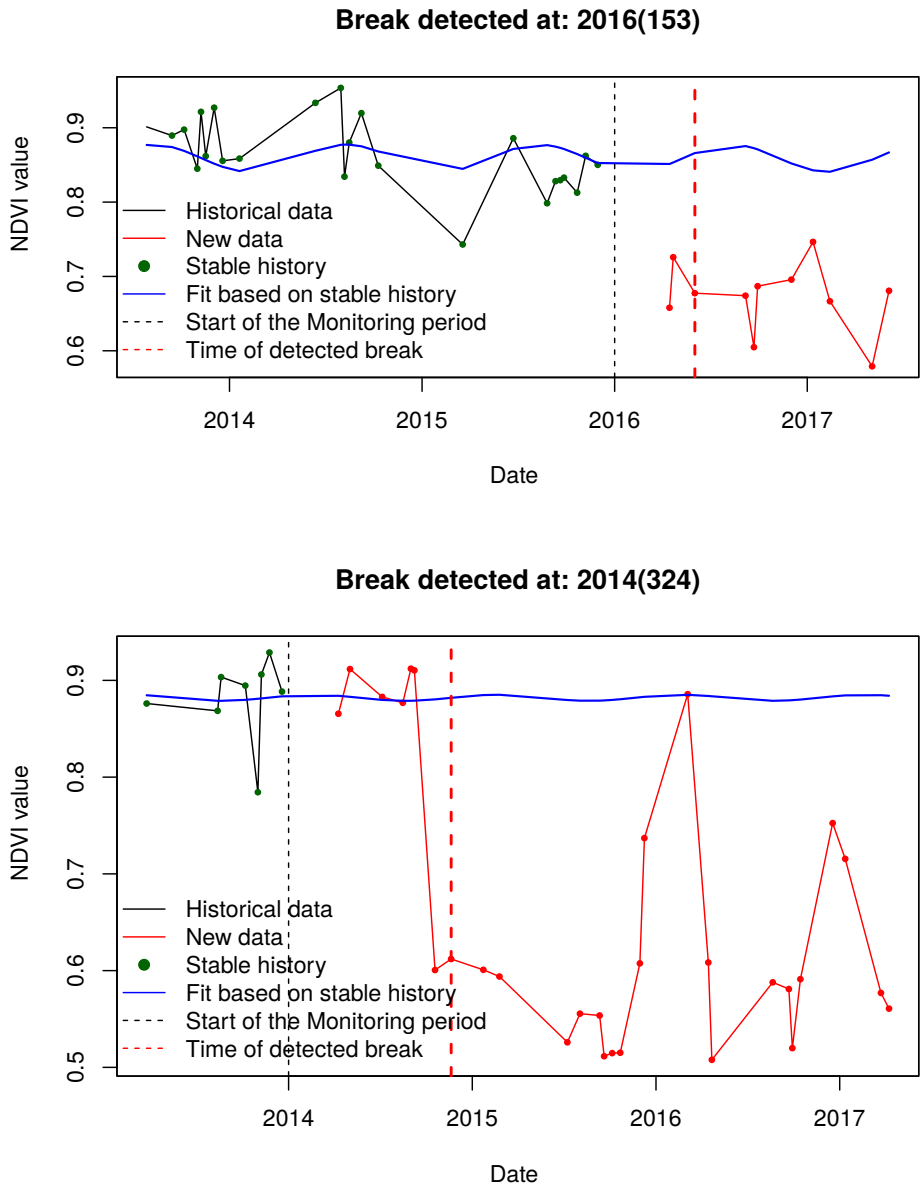

Figure 4.6: BFAST Monitor analysis of Landsat 8 OLI NDVI time series in the Guyana 2017 study site. Top: the central pixel of a log deck built in 2016. Bottom: a pixel on a road built in 2014. The increase visible in 2016 is due to the shifting of the road one pixel to the north in that image, which could be due to georeferencing issues or different sun-sensor angle.

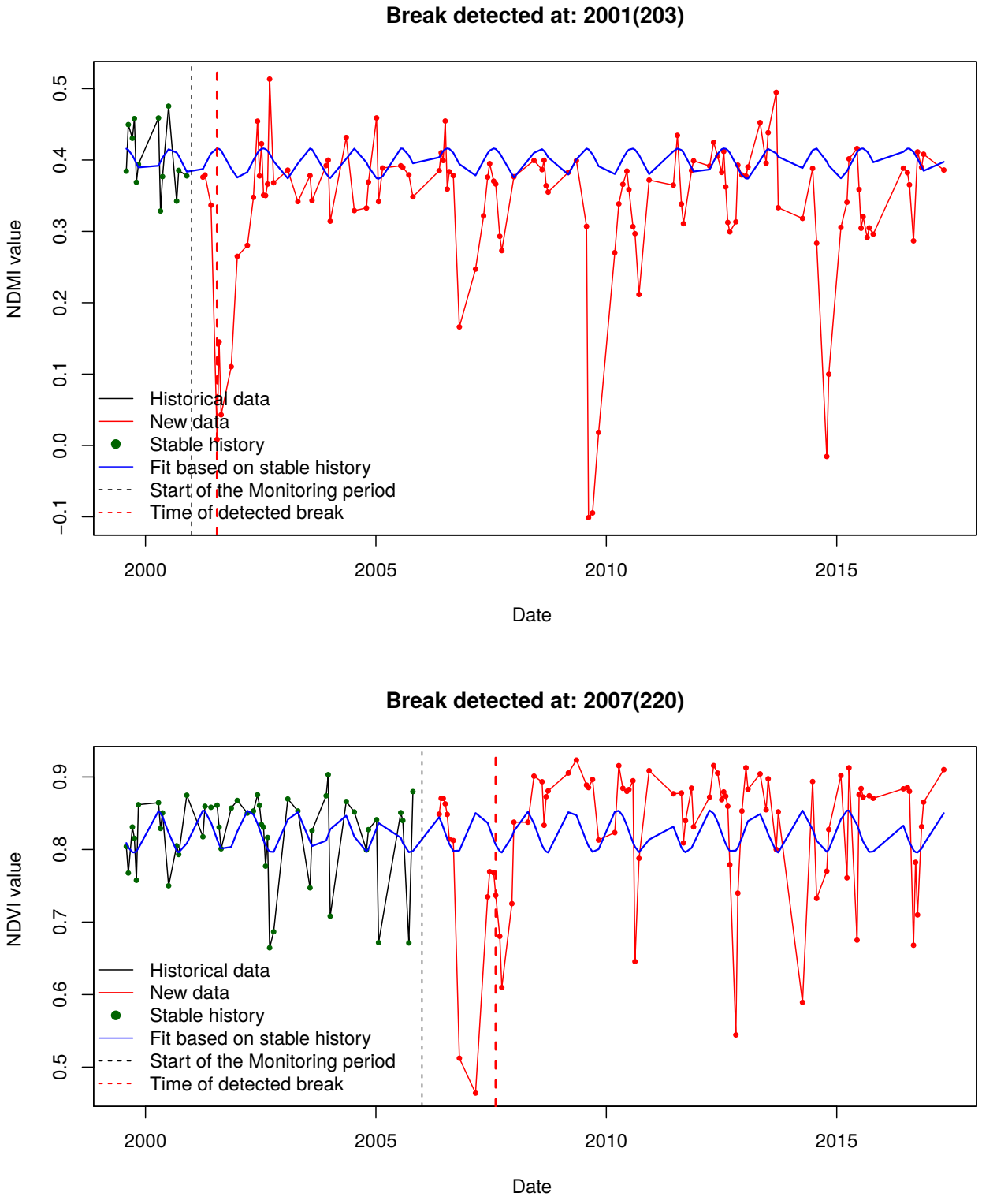

Figure 4.7: Landsat 7 ETM+ time series of a pixel in a shifting cultivation plot in the Peru study site. Top: NDMI. Several disturbance and regrowth cycles are visible and the first one is detected by BFAST Monitor. Bottom: NDVI. Only the largest disturbance is visible and is detected, but the NDVI values after the disturbance are higher than before it. The negative outliers in 2010-2015 are cloud shadows that influence NDVI values but not NDMI.

their pre-disturbance values; after that point, NDVI values exceed those of the original undisturbed forest (see figure 4.7, bottom).

4.2 Vegetation index comparison

For treefall gap detection, as discussed in section 4.1.1, there were significant differences in means before and after a selective logging event in all of the tested vegetation indices. However, the magnitude of change differed among the vegetation indices (see figure 4.3), and so did the ability to detect larger logging features such as logging roads and log decks (see figure 4.7).

4.2.1 NDVI

NDVI was found to be less sensitive to changes in forest structure than the other vegetation indices tested; on average NDVI values in pixels covering treefall gaps decreased from 0.80 to 0.74 (see table 4.2). In cases where the forest floor consisted mainly of non-photosynthetic vegetation or bare soil, or if the forest floor was damaged, NDVI was a reliable indicator of treefall gaps and other logging features (see figure 4.6), however, fewer gaps can be seen in NDVI than in other vegetation indices (see figure 4.8). In other words, if a gap was visible in NDVI, it was clear that it was a treefall gap, but not all gaps were visible in NDVI.

One unique property of NDVI was found to be its relation to shadows. Since NDVI is a ratio of the reflectance in the red band and the reflectance in the NIR band, when vegetation is shadowed (e.g. by a cloud shadow of a shadow from a neighbouring tree), the reflectance in red becomes close to 0 and thus NDVI becomes close to 1. Thus forests all appeared to have high NDVI values (0.8-1.0), except where there were gaps in the canopy. In addition, land cover change (such as from forest to grasslands or silviculture) changed the mean NDVI value, as seen in figure 4.7. Whether the change was an increase, decrease, or a change in seasonality depended on the properties of the new land cover type.

4.2.2 NDMI and NBR

The SWIR-based vegetation indices NDMI and NBR were the most sensitive to changes in forest structure from all the vegetation indices tested, as seen in figure 4.3. After a logging event, mean NDMI values in affected pixels decreased from 0.30 to 0.15, whereas NBR values decreased from 0.60 to 0.48. The relative magnitude of change was higher in NDMI than in NBR. NDMI values differ more within forests, revealing their structure, whereas NBR tends to vary less within forests but highlight only particularly large disturbances (see figure 4.8). However, the two indices are highly correlated with one another (Pearson's correlation: 0.94), as the only difference between them is the choice of the SWIR wavelength.

The SWIR-based indices turned out to be highly sensitive to internal shadows within forests, but insensitive to cloud shadows, because unlike the red band, NIR values are higher than zero when a cloud shadow is over vegetation, and cloud shadows reduce the reflectance in NIR and SWIR almost equally. This is a useful property, because it allows the use of pixels that for other vegetation indices would not be useful, and it also helps when the cloud shadow masks are not perfectly reliable (as is often the case). Sensitivity to internal shadows comes from the NIR band, whereas the SWIR band is smooth and does not capture internal shadows, but is good at capturing the high reflectance from bare soils.

One issue of calculating NDMI and NBR is that the SWIR band often times has a coarser resolution than the visible and NIR bands due to lower amounts of energy returned from the land surface at

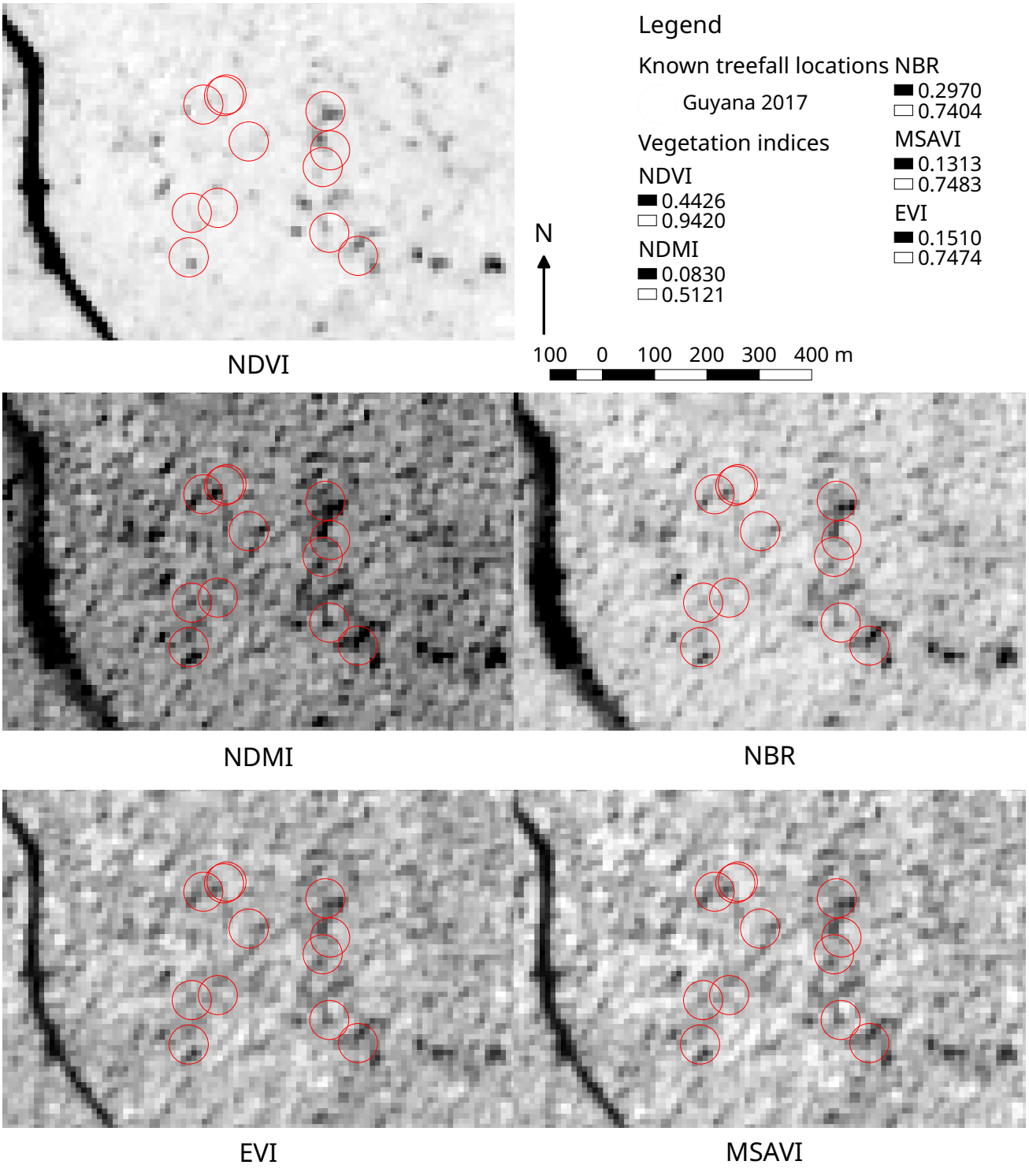

Figure 4.8: Comparison of the five vegetation indices derived from a Sentinel-2 MSI image of February 12, 2017, less than a month after the selective logging event.

those wavelengths. This is the case in Sentinel-2 and ASTER imagery. Therefore in order not to lose information from the NIR band, the SWIR band data has to be upsampled to match the NIR band pixels. This can be done by using nearest neighbour interpolation or bilinear interpolation. Testing of both interpolation methods revealed that in forests, nearest neighbour resampling leads to block artefacts and could be misleading, whereas bilinear interpolation was more appropriate, however the differences are overall small for gaps. The largest differences were within logging roads, where the road outlines would become blurred when using bilinear interpolation and blocky in a salt-and-pepper pattern when using nearest neighbour interpolation.

4.2.3 EVI and MSAVI

The other two vegetation indices tested, EVI and MSAVI, are both complex indices that were designed to overcome the deficiencies in NDVI. Even though the approaches differ, the result is largely the same: both vegetation indices are highly correlated in forests (Pearson's correlation: 0.94). The two indices are in between NDVI and the SWIR-based indices in sensitivity: they capture bare soils and non-photosynthetic vegetation like NDVI does, and are sensitive to internal shadowing like the SWIR-based indices. However, they are less sensitive to either compared to the other types of vegetation indices, thus the overall sensitivity to selective logging events is rather poor (see figure 4.3).

EVI is unique in that it compensates for the presence of thin clouds and cloud edges. This is a useful property, since while most cloud masking approaches are good at detecting thick clouds, thin ones are much more difficult to detect. However, unlike the SWIR-based indices, EVI is affected by the presence of cloud shadows. EVI was also the vegetation index that is least correlated with any of the others except MSAVI: 0.68 correlation with NDMI and 0.69 correlation with NDVI and NBR.

MSAVI is highly correlated with EVI, and the main difference between the two is that MSAVI does not share the property of atmospheric noise correction and thus is affected by light clouds. On the other hand, only the red and NIR bands are required to calculate MSAVI, whereas EVI also requires the blue band, which is not always captured (e.g. by ASTER).

5 Discussion

5.1 Selective logging feature detection

5.1.1 Detection possibilities

The results showed that the ability to detect selective logging treefall gaps from Landsat imagery is extremely limited, which confirms the findings of Asner et al. (2002) and Asner et al. (2004). Even when the location and appearance time of the canopy gap is known, the 30 m resolution of Landsat is not enough to reliably detect changes, neither in an automated way nor manually. While the tree crown size in the Amazon rainforest tends to reach 30 m in diameter, it is very rare that the pixel grid would align with the gap left by logging a particular tree. The more common case is for the gap to be split into two or four pixels, in which case the effect that the logging event has to vegetation index values is too low to be discernible due to the influence of the surrounding untouched vegetation.

However, the results showed that the 10 m resolution of Sentinel-2 MSI is enough to visually detect most treefall gaps, and that it should be possible to detect the gaps in an automated way in the future, when Sentinel-2 imagery time series grow in length so as to allow using time-series-based detection methods. The identified treefall gap size did not significantly correlate with the DBH of the felled tree, unlike ground measurements are known to (Jackson et al., 2002), however, the sample size was too small to draw conclusions. This shows that more research is needed to better understand the use of Sentinel-2 MSI imagery for treefall gap detection once the imagery archive length increases, as well as to better identify the relation between tree size and treefall gap size using a larger sample of trees.

From the other selective logging features identified by Asner et al. (2002), skid trails were not identifiable from any of the satellite imagery used, whereas large logging roads and log decks were both identifiable and automatically detectable from both Landsat and Sentinel-2 imagery. These findings are similar to those of Read (2003).

All in all, logging features that were possible to detect were:

1. **Moderate size gaps in dense forests with a soil background**: If the forest floor is bare soil or non-photosynthetic vegetation, as in Guyana 2017 study site, then the treefall gaps are identifiable by a change in NDVI (see figure 5.1, case B). This is due to photosynthetic vegetation strongly absorbing light in the red band and strongly reflecting light in the NIR band. These types of gaps are also discernible visually by inspecting the NDVI values, as fresh treefall gaps are small and thus stand out from intact forest. However, they do not stay visible for long due to canopy and forest floor regrowth.

2. **Small gaps in dense forests**: If the treefall gaps are too small to cover a pixel size area, or if the forest floor is vegetated, the gaps can still be identified indirectly using NDMI due to a shift in the forest texture, as new internal shadows from nearby trees appear on the edges of the newly created gap (see figure 5.1, case C). This allows for identifying selective logging of smaller trees, however, it is an indirect indicator of gaps. Shadows may also shift due to sun-sensor angle geometry, potentially confounding automated detection algorithms.

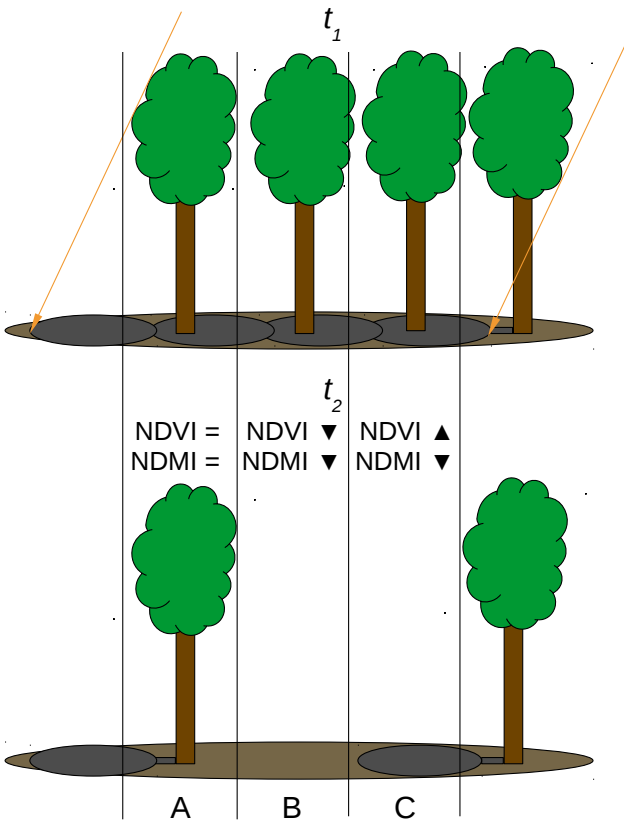

Figure 5.1: A simple theoretical 2D model of changes in vegetation indices in a forest following selective logging of two trees. Orange arrows indicate the sun zenith angle, black lines indicate pixel boundaries of a nadir-facing satellite sensor. At timestep t_1 all three pixels have high NDVI and NDMI values. After logging at timestep t_2, pixel A has high NDVI and NDMI, pixel B has low NDVI and NDMI, pixel C has high NDVI but low NDMI values. In case of a smaller gap, pixel B would have the same values as pixel A, and so NDVI would not be useful for gap identification.

3. **Logging roads**: Detecting the presence and the building time of logging roads was possible in an automated fashion in the Guyana 2017 study site using Landsat imagery. This is in line with other studies on logging roads (Kleinschroth et al., 2016). However, new roads were built only in one of the three study sites. The other two sites were in close proximity to an existing major road, which is convenient for carrying out selective logging because no new road construction is needed. Therefore while it is useful to detect logging roads and they are one of the easiest logging features to identify using automated time series methods, roads alone are not sufficient to locate all cases of selective logging nor to estimate the intensity of the performed selective logging.

4. **Clear-cuts**: When deforestation happened as part of slash-and-burn agriculture or shifting cultivation, as the case was in the Peru study site, it was possible to identify using methods based on time series in an automated way. Since the area that is affected is large, Landsat imagery can be used for this purpose, and its long archive is advantageous for analysing the imagery using time series methods. In case of tree plantations or shifting cultivation, these methods can be used to determine the time it takes for the canopy to regrow and reach pre-harvest levels, though the estimates depend on how fast the vegetation index used saturates (see figure 4.7). However, this type of logging is already relatively well-understood and is not usually considered to be selective logging.

While detecting these logging features from satellite imagery was possible, doing so is nonetheless a challenge due to the complexities involved. A number of scenarios under which automatic detection of treefall gaps would become more challenging or give erroneous results have been identified in this thesis. The causes of these scenarios fall under two categories: vegetation change issues and issues with satellite imagery itself.

5.1.2 Detection challenges related to vegetation change

The first detection challenge is posed by the effects of vegetation seasonality. In the Amazon region, both deciduous and evergreen trees mix, and deciduous trees may not have the same leaf senescence cycle across different species. Individual trees that had dropped their leaves have lower NDVI values (and show up as white in true colour imagery) and are typically surrounded by trees with intact leaves. As such, they may not be easily distinguished from treefall gaps; even the fact that the leaves of such trees regrow next season may not be a good differentiator, since canopy regrows rapidly after selective logging too. Time series methods are supposed to be able to deal with such seasonality by use of seasonal models, however, this assumes the availability of sufficient stable history to determine a pixel's seasonality, and that the pixel is homogeneous (covers only a single tree) and its area covered is constant (perfect coregistration of images).

The second challenge is that while the methods employed here are suitable for detecting gaps in dense forests, they might not be suitable for sparser forests whose understory receives a sufficient amount of light to be photosynthetic, or for stand-alone trees. In those cases, the logging event would not have an effect on the vegetation indices. The most notable change in this scenario would instead be the disappearance of the shadow of the logged tree, which would increase NDMI rather than decrease it. This issue may be compounded by seasonality issues (logging a leafless tree in a sparse area would also increase NDVI), and RIL schemes may also preclude the creation of visible logging roads and decks in such areas.

The third challenge that was identified is selective logging happening next to an existing gap. Especially in RIL, if a gap or logging road already exists next to a tree slated for logging, it will be felled in the direction of the existing gap or road. The result is that a new gap does not appear.

The existing gap may widen, but the change would be subtle compared to the usual case of logging creating an entirely new treefall gap.

The fourth challenge relates to logging targets: in some cases, the trees slated for logging may not be the ones occupying the upper layer of the canopy, but rather be in the understory. This was the case in the Guyana 2017 study site, where multiple trees of different sizes would be cut, not necessarily only the largest ones. In such a case, no change would be visible from optical remote sensing imagery at all, since the canopy of taller trees would cover such an event up, similar to how it covers skid trails.

5.1.3 Detection challenges related to satellite imagery

The spatial resolution of a sensor and the division of the raw data into pixels has an effect on what area a given pixel covers. The coarser the resolution, the larger the area that is integrated over to obtain the reflectance value, which dilutes the effect of a logging event. The effect is made worse if the canopy of a particular tree falls on the boundary between two or even four pixels, since the integrated area doubles or quadruples in such a case, effectively making it impossible to detect such a logging event. At a resolution of 10 m (100 m^2 area), there is a reasonable chance that at least one pixel will fall within the crown of a single tree or exclusively within a newly created treefall gap, but at a 30 m resolution (900 m^2) this chance is much lower. As such, whether the logging of a particular tree can be detected may come down to luck of whether the pixel grid aligns favourably or not. In addition, good coregistration of images is important for time series methods; if the images shift by a pixel in between acquisitions, one observation in the time series may refer to a completely different neighbouring tree compared to a subsequent observation.

Another issue with optical remote sensing imagery is the cloud cover, which is very frequent over the Amazon and especially during the rainy season. Dense clouds obscure the tree canopies, whereas light clouds and cloud shadows change the reflectance values. Different vegetation indices react differently to such atmospheric effects: NDMI and NBR can largely compensate for cloud shadows, EVI can compensate for light clouds and cloud edges, whereas the other tested indices are affected by both. Compounding the problem is unreliable cloud and cloud shadow detection algorithms employed by different preprocessing methods. While the `fmask` algorithm for Landsat data continues to be refined (Zhu et al., 2015; Qiu et al., 2017), it is not yet reliable enough to mask all instances of clouds and cloud shadows (e.g. see figure 4.7, bottom: the single-date downward spikes of lower NDVI values are all caused by cloud shadows, but may be detected as logging events; the time series includes only the pixels marked as completely clear in the quality control layer). While temporal outliers could be removed using temporal filtering methods, it would also risk removal of true selective logging effects.

Imagery archive length is an issue as well. While Sentinel-2 MSI imagery was found to be sufficient to detect larger treefall gaps, its archive only dates back to late 2015. Given cloud cover, this was not enough to build a stable history for time series analysis. The same issue occurred with Landsat 8 OLI data in the Peru study site: while there were enough points for the algorithm to attempt analysis, the history was too brief and so the algorithm reported numerous false positives. The archive lengths are always growing, so the situation is expected to get better in the future (especially for Sentinel-2, with the launch of the Sentinel-2B satellite in 2017), but the detectability of historical selective logging events will largely stay as it is now.

Lastly, while time series analysis is powerful and the increasing lengths of pixel times series allows for more opportunities of detection, it comes at a cost of very large volumes of data that have to be processed. For example, Sentinel-2 MSI imagery before the end of 2016 is available in collections of granules with a download size of around 5 **G**ib**ib**ytes (GiB), and after that in single granules with a size of around 0.5 GiB. A full time series consisted of 70 such granules. Landsat imagery was

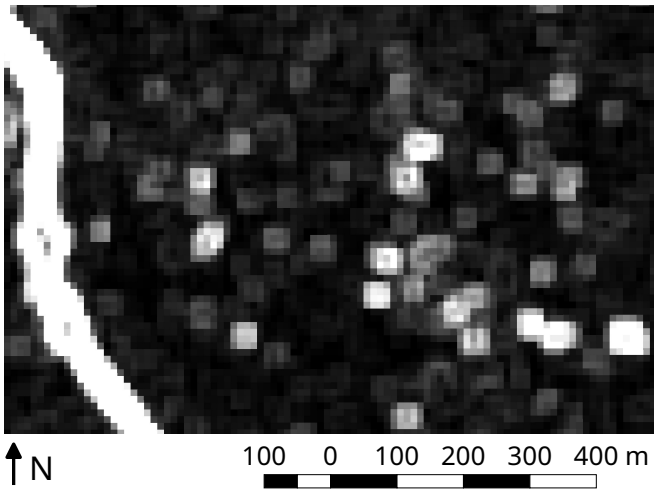

Figure 5.2: Texture analysis of the Guyana 2017 study site Sentinel-2 image of February 12. Black corresponds to a standard deviation in NDVI of 0.0044, white to 0.0921 in a 3 by 3 pixel moving window.

smaller, with around 0.3 GiB download for 5 vegetation indices per tile, but the time series was much longer, with 731 tiles of ETM+ and 179 tiles of OLI imagery to process for the Peru study site alone. Intermediary results of each processing step had to be stored for algorithm validation purposes as well, multiplying the disk space required. The imagery was processed using an 8-thread Intel Core i7-3770 processor with 16 GiB **R**andom **A**ccess **M**emory (RAM), and yet it took around a week to download and preprocess the time series of a single sensor for a single study site. In addition, some preprocessing steps had high RAM requirements, for instance, the Sentinel-2 atmospheric correction software `sen2cor` required over 8 GiB of RAM to process a single granule, precluding the ability to process several granules at a time on this hardware.

5.2 Comparison of vegetation indices

Of the five vegetation indices tested (NDVI, NDMI, NBR, EVI, MSAVI), three groups were identified according to how the indices perform in forests and what changes are evident when a selective logging event occurs. The sensitivity to selective logging features and other properties of the indices differed (see figure 4.8), and a combination of several indices may be advantageous for detection purposes.

5.2.1 NDVI

NDVI was unlike other vegetation indices tested in that shadows cause high rather than low values of the vegetation index. This makes NDVI especially useful for initial detection of selective logging treefall gaps. As long as the background behind the canopy is non-photosynthetic and the gap size compared to sensor spatial resolution allows for it, gaps in NDVI stand out clearly from the surroundings. Forests appear rather homogeneous in NDVI, since internal shadowing causes an increase in NDVI, but a small one, since NDVI is close to saturation (0.85-0.95) in forests in the first place. A gap with a soil background visible causes a marked decrease in NDVI.

One possible application for NDVI in treefall gap detection would be in spatial texture analysis. Asner et al. (2002) used variance in a 3 by 3 pixel moving window on Landsat ETM+ imagery as an indicator of texture, and while it did not result in useful detection of treefall gaps, it could be useful in combination with Sentinel-2 MSI imagery (see figure 5.2, cf. figure 4.1). There is a number

of spatial texture analysis methods, such as the median above 90th percentile used by Hamunyela et al. (2016), and more research is needed to determine the most appropriate method specifically for treefall gap detection.

5.2.2 NDMI and NBR

While NBR is a highly popular index for logging detection (Shimizu et al., 2017; Schneibel et al., 2017), the related NDMI had a more pronounced change in values after a selective logging event, the most of all indices tested (see figure 4.3). Thus NDMI is the most useful single vegetation index for detecting selective logging events of all the ones tested in this study.

Furthermore, neither NDMI nor NBR are affected by cloud shadows, therefore more data can be used (fewer pixels need to be discarded) when analysing these indices. NDMI is also less affected by thin clouds compared to other indices, with the exception of EVI. This is a major advantage in the Amazon region, where cloud cover is frequent, and was also useful in the cases when the built-in cloud and cloud shadow detection algorithms for satellite imagery products failed to detect thin clouds and cloud shadows properly.

However, while NDMI is highly sensitive to logging events, it is important to keep in mind that its sensitivity to internal shadows is at least as strong as the sensitivity to newly appearing bare soil. This property of NDMI is in part the reason why it is sensitive to selective logging events in the first place, as trees with a small crown that get logged may only be detectable by shift in shadows. But this means that there is a risk of false positives caused by internal shadows shifting due to a change in sun-camera angle geometry in between image acquisitions, rather than real logging events. Thus for methods based on time series, images taken at similar solar angles are necessary for consistency when using NDMI or NBR. Another issue with these vegetation indices is the need for SWIR bands that are often available at a lower spatial resolution than the visible and NIR bands. Bilinear interpolation was found to work well for upsampling Sentinel-2 SWIR bands, but at a cost of blurring roads.

One way to get the best of both NDVI and NDMI could be to use NDVI for detecting the larger selective logging features (newly built roads and log decks, large treefall gaps) in order to detect the presence of a selective logging operation in an area, and then use NDMI to detect the smaller treefall gaps in order to determine the intensity of the selective logging operation within the area.

5.2.3 EVI and MSAVI

EVI and MSAVI have been found to be sensitive to both internal shadows and bare soil, but less sensitive to shadows than NDMI and less sensitive to bare soil than NDVI. This makes EVI and MSAVI less useful than the other vegetation indices tested, since the treefall gaps do not stand out from natural internal shadowing of a forest when looking at the spatial pattern, and the difference in values before and after logging from time series is low compared to other vegetation indices (see figure 4.3). The main useful property of EVI is that it compensates the effect that thin clouds (but not cloud shadows) have on the vegetation signal underneath, whereas the main useful property of MSAVI is that it only requires the red and NIR reflectance bands, so it can be derived from sensors that capture few optical bands.

5.3 Comparison of sensors

Three types of sensor imagery were analysed in this study: Landsat (ETM+, OLI) 30 m, Sentinel-2 MSI 10 m, and ASTER 15 m. See figure 5.3 for a side-by-site comparison. In addition, 0.5 m

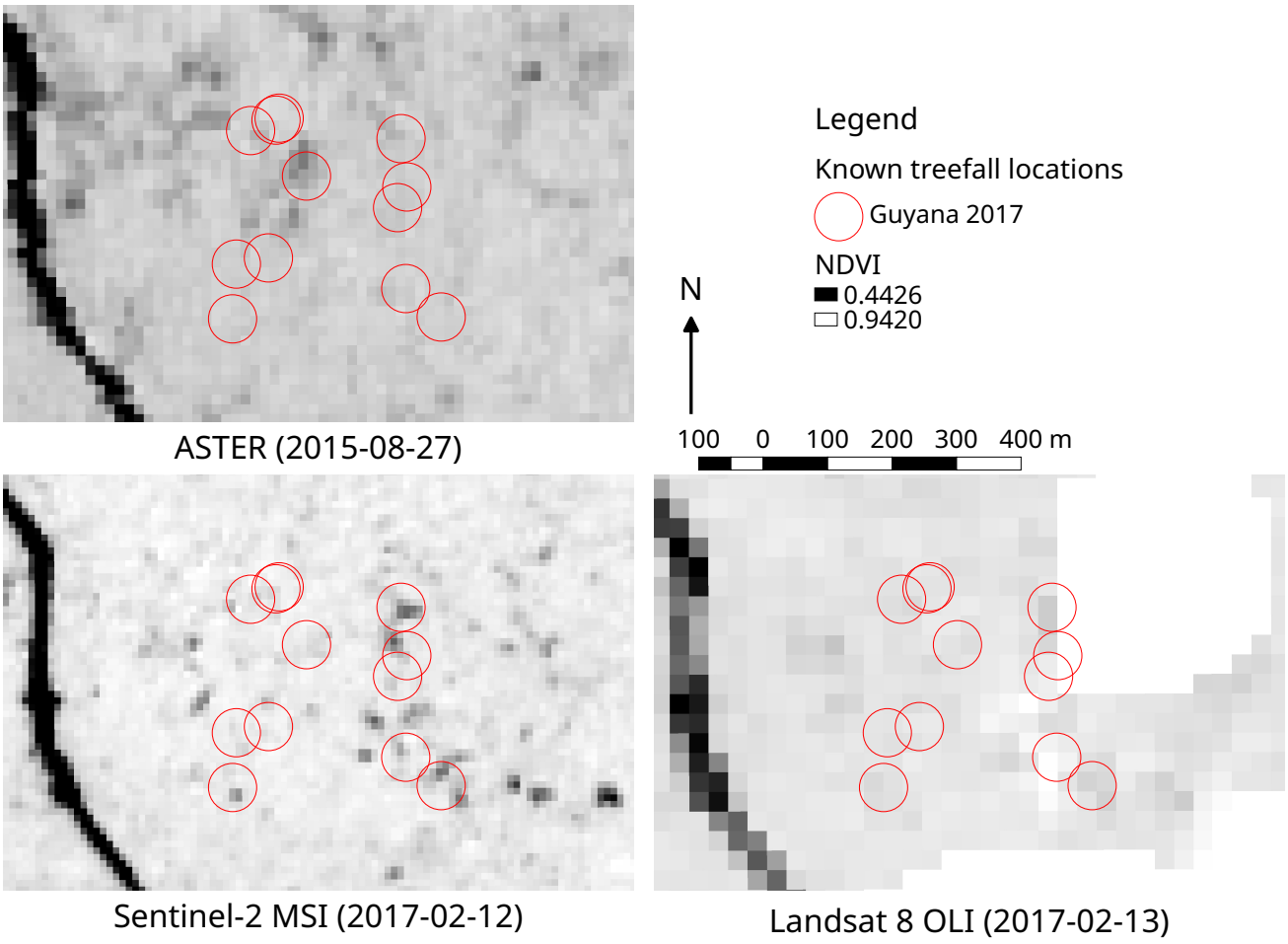

Figure 5.3: Comparison of NDVI derived from different sensors in the Guyana 2017 study site. The Sentinel-2 MSI and Landsat 8 OLI images were taken immediately following the selective logging event, the ASTER image was taken two years prior (more recent images are clouded). The completely white areas in the OLI image are masked out cloud shadows.

resolution imagery from DigitalGlobe was used for validation. Each types of imagery have their own strengths and weaknesses.

Landsat imagery has the coarsest resolution, which is insufficient for detecting treefall gaps. However, it has the longest archive and a short revisit time, which makes it ideal for detecting larger selective logging features, such as major roads and log decks. It is also well suited for detecting agriculture encroaching upon previously intact forests and other land cover changes. Thus Landsat imagery can be used to quickly assess whether a (selective) logging campaign is underway in an area (Frolking et al., 2009). However, it is unsuitable for quantification of the selective logging intensity, since even though the area occupied by roads and log decks is correlated to the selective logging intensity (Jackson et al., 2002), it does not correspond to the actual volume of wood cut linearly, but rather levels off (Broadbent et al., 2006).

Sentinel-2 MSI imagery has the finest resolution, which is sufficient for detecting most treefall gaps. However, it lacks in history in order to do so automatically at this point in time, since the archive only goes back to the end of 2015, and there is very frequent cloud cover over the Amazon that lowers the available number of observations. One solution would be to wait until the history grows longer. In that case, only treefall gaps starting from the end of 2017 or later will be detectable. Another solution would be to attempt to calibrate other sensors, such as Landsat, to Sentinel-2 imagery for use as historical reference. However, such a task would be rather complex and potentially error-prone, as sun-sensor angle geometry as well as spatial and spectral resolutions do not match.

ASTER imagery is of intermediate resolution and the archive goes back to 1999, matching Landsat 7. However, the revisit time is long, making this type of imagery only suitable for before-and-after comparisons. The saturation of the SWIR sensor in 2008 and the small range of digital numbers further lowers the utility of ASTER images for detecting selective logging. However, it is useful for Landsat imagery validation purposes, since 15 m resolution is enough to distinguish forest texture and individual trees in clearings.

Very high resolution imagery has the same limitations as ASTER: the revisit time is even longer and fewer bands are captured. It is useful for validating treefall events and adjusting location data collected in the field using a Global Navigation Satellite System, since the canopies of individual trees are visible. Read (2003) used very high resolution Ikonos imagery and could also distinguish larger treefall gaps and skid trails (which are not visible in any other imagery).

All in all, 10 m resolution like that of Sentinel-2 MSI is a good starting point for selective logging detection and monitoring, since it allows for a frequent revisit time needed for time-series-based methods, and allows for detecting treefall gaps, which is a direct measure of selective logging intensity.

5.4 Comparison with other studies

Detection of selective logging from satellite imagery has been attempted by several authors in the past. One of the first such attempts was by Asner et al. (2002). The authors concluded that Landsat 7 ETM+ spatial resolution was insufficient to detect treefall gaps and skid trails (even when using spatial texture analysis) and may be sufficient to detect log decks and roads depending on the type of logging operation. These conclusions are fully in line with the findings in this study; log decks could be identified in the Guyana 2017 site, but not in the two others due to the proximity of existing roads which lowers the need for constructing log decks. In a follow-up study, Asner et al. (2004) evaluated the use of spectral unmixing on the same Landsat 7 ETM+ imagery in order to increase sensitivity to selective logging events, and concluded that spectral unmixing helps with detection of all types of selective logging features. However, in the cases of RIL forest plots one year after logging, the unmixed forest canopy fraction in treefall gaps and skid trails was still little different (>90%) than

that of pristine forest (>95%). In addition, spectral unmixing requires a large library of endmembers (samples of reflectance in pure pixels of a class) of the desired classes to be unmixed. Furthermore, nowadays there are new fuzzy classification methods based on machine learning that can make use of more than just reflectance data, which have the potential to increase the separability of treefall gaps in Landsat data. On the other hand, the use of higher resolution imagery like that of Sentinel-2 MSI may make such methods unnecessary altogether.

A year after the last publication, Asner et al. (2005) developed a proprietary software package called CLAS for performing large-scale deforestation and forest disturbance analysis based on the aforementioned spectral unmixing method using Landsat 7 ETM+ imagery. The authors found that their estimates of logged timber volumes were much higher than the previous studies had estimated. However, given the difficulty of detecting treefall gaps and skid trails from Landsat imagery in RIL plots, the estimates achieved are still likely to have been conservative.

Read (2003) compared Ikonos 1 m and 4 m resolution imagery with Landsat 7 ETM+ and concluded that 1 m resolution was sufficient to identify most of the selective logging features (most, but not all treefall gaps), whereas 30 m resolution was only sufficient for identifying major roads and log decks. This is also in line with the findings in this study, as well as the findings of Asner et al. (2002). DigitalGlobe imagery that was used in this thesis allowed the identification of individual trees that have been cut down, but not treefall gaps per se, since the time of acquisition is several years apart and the treefall damage is regenerated over this time.

Broadbent et al. (2006) attempted to identify known treefall gaps in RIL sites using NDVI and spectral unmixing of 30 m ASTER imagery. The authors concluded that both NDVI values and the photosynthetic vegetation fraction from spectral unmixing were significantly affected by the selective logging event in all sizes of treefall gaps. This conclusion would appear to be inconsistent with both that of the previous studies mentioned here, and the results of this thesis. However, the magnitude of change in NDVI directly after harvest in small and medium gaps was reported to be from -0.01 to -0.015. This change is very small, and indeed at the edge of the digital number sensitivity of the ASTER sensor: a change in 0.01 of NDVI corresponds merely to a change in 5 digital number values. Variations in NDVI in residual forest over time were also shown to be around -0.01 in magnitude. This suggests that while there are differences in NDVI values even in small gaps after logging, the difference is not higher than natural variability and thus automated detection of treefall gaps using 30 m resolution imagery is not feasible after all. The magnitude of change in the photosynthetic vegetation fraction was shown to be higher, but the same caveats as in the previous spectral unmixing studies apply.

More recently, a number of publications have attempted to automate seletive logging detection by using time series methods, most commonly using the software LandTrendr (Kennedy et al., 2010). Fragal et al. (2016) analysed NDVI time series in LandTrendr in order to detect changes in forest cover and differentiate between natural and anthropogenic forest disturbances in the Amazon region, but focused on large disturbances rather than selective logging. Shimizu et al. (2017) used NBR in order to detect selective logging in Myanmar using Landsat data, however, the authors did not specify what they consider as the definition of selective logging: log decks, roads, treefall gaps and/or skid trails. Any disturbance detected by LandTrendr was labelled as selective logging; however, the results of this thesis and previous studies show that only deforestation, logging roads and log decks are detectable from Landsat imagery, therefore the LandTrendr output very likely indicated only these indirect measures of selective logging intensity which do not necessarily indicate the actual scale of the selective logging operations like treefall gaps would. The validation in that study was restricted to comparisons of detected disturbance intensity with reported logging intensity within forest blocks, which makes it unlikely that the detected disturbances also included treefall gaps.

Another attempt at detecting selective logging using Landsat data using the spectral unmixing

method was done by Grecchi et al. (2017). The obtained vegetation fractions were analysed in grid cells of 300 m, and there was no distinction made between the different logging features. Whether a cell is considered to be selectively logged was determined only by the intensity of disturbances, validated by analysis of the same Landsat imagery. Given the results of this thesis, only the logging roads and log decks would have been detected, therefore only an approximation of the area affected by selective logging was obtained. Without knowledge of logging intensity, the area measurement alone is not necessarily indicative of the harvested timber volume nor of the effect on the forest ecosystem, and the threshold at which a cell was considered to be selectively logged rather than deforested is likewise arbitrary.

All in all, studies so far have shown that it is not feasible to detect treefall gaps nor skid trails using 30 m resolution data, only logging roads and log decks that are not necessarily indicative of logging intensities. Thus the findings of this thesis that detecting larger treefall gaps using 10 m resolution Sentinel-2 data is possible is an important step towards much more precise estimations of the impact of selective logging. The literature comparison also revealed the importance of understanding and explicitly stating what logging features (logging roads, log decks, treefall gaps, skid trails) are necessary for the author to consider an event as selective logging, since otherwise the results between different studies are incomparable. The importance of validation using independent validation data should also be stressed.

5.5 Recommendations

For further research, there are a number of areas that could be improved in order to further advance the ability to automatically detect selective logging events from remote sensing data.

First of all, the availability of validation data is very important. In order to draw better conclusions, more data from larger selective logging field campaigns would be needed, with more observations of logged trees and their logging gaps. The locations of the logging gaps and other logging features, their size, the size of the logged trees and such are all valuable data that could give further insight in what is possible to detect and what is not. Given the results in this thesis, validation data specifically from selective logging campaigns from 2017 onwards would be the most useful due to the availability of Sentinel-2 MSI imagery. The availability of more imagery from higher-resolution sensors (such as ASTER, Ikonos, SPOT) would also help validate the results of a selective logging detection attempt.

Extra processing for cloud masking, or improved methods for cloud masking, would help create consistent time series. Since different vegetation indices can deal with certain types of clouds or cloud shadows, different masking approaches for specific vegetation index types would allow making use of partially clouded or shadowed pixels where they can be used, maximising available observations, and masking out cloud influence for vegetation indices that cannot make use of such pixels. Temporal cloud masking (discarding single-date negative outliers), masking based on spatial context such as sNDVI (Hamunyela et al., 2016), or a combination of these methods might also improve methods based on time series, however, it might also lead to discarding selective logging events as well. All of these extra processing steps would also require more processing power and storage.

Improvements to the cloud masks provided in the quality control layers of satellite imagery products would benefit all users of the imagery. There are several approaches to cloud masking available, such as using thresholds of cloud indices to predict the presence of clouds (such as done by `fmask` or PROBA-V quality control) or using machine learning to classify pixels as clouded or not (such as done by Sentinel-2 `sen2cor` software). More research is needed to identify the best option, or a combination of options, and to apply this knowledge to improve cloud masking for all the sensors.

In order to improve the ability to detect treefall gaps, more approaches can be tested. There are

additional vegetation indices such as tasselled cap transformation, Normalised Difference Fraction Index (Souza et al., 2005), Transformed Chlorophyll Absorption Ratio (Haboudane et al., 2002), etc. that can be tested for suitability to detect treefall gaps. Spatial features such as various forms of texture analysis and normalisation based on neighbouring pixels can also be tested, in order to see whether making use of information in the surrounding pixels in time series analysis, rather than looking at pixels individually, improves detectability. Trees neighbouring the site of a logged tree are likely to have had similar changes in reflectance over time before the logging event, and divergent ones after the event. However, unfiltered cloud cover or cloud shadows may also cause differences in time series even in adjacent pixels.

Another option for detecting treefall gaps and other logging features, perhaps even from Landsat imagery, would be to extend the spectral unmixing approach suggested by Asner et al. (2004) into a fuzzy classification approach using machine learning methods. Such an approach would be able to make use of all optical bands at once, as well as auxiliary data such as time series metrics, spatial context, data from other sensors etc. and be possible to train on mixed pixels rather than assuming a linear mixture. Such a trained fuzzy classification model could then be used to predict either the location of treefall gaps directly, or a well-understood intermediary variable such as f_{Cover} that has a direct relation with canopy gaps (such as done by Bacour et al. (2006)) in order to attempt to locate the gaps using this variable.

One other option would be to make use of satellite imagery that is of even finer resolution than 10 m, such as that of the PlanetScope satellite constellation (which would be suitable for time series analysis due to a short revisit time), Ikonos, QuickBird, GeoEye or other such satellites with very high resolution sensors. At such spatial resolution, a tree canopy is represented by several pixels, so object-oriented methods would be necessary to analyse such data, but it would allow tracking individual trees over time by coregistering the unique canopy shapes and relations to neighbouring trees between subsequent acquisitions and detecting any changes to the forest layout over time. The downsides of using such an approach is the massive amounts of data that would need to be processed, and the fact that most of the very high resolution imagery products are commercial and thus not freely available.

Imagery from radar or lidar sensors could be either an alternative to optical imagery or used together. Radar imagery would be useful in areas such as the Amazon due to its property of penetrating clouds, and the various beam polarisations giving information about the structure of the objects on the ground. A time series of radar imagery, such as from the Sentinel-1 satellites, would be more consistent than optical imagery, barring speckle effects. Spaceborne and airborne lidar data would also be useful for determining canopy structure changes; a shift in canopy height would be a good indication of a selective logging event. However, currently there are too few operational spaceborne lidar sensors, whereas airborne lidar campaigns are costly and thus lidar data is updated infrequently.

Lastly, data from multiple sensors, optical or otherwise, could be fused to enhance time series of a specific location. For instance, Landsat 7 ETM+ and Landsat 8 OLI imagery have the same spatial resolution and mostly the same optical bands, so imagery pooled together can be used to make time series denser. However, images still need to be calibrated across sensors, since either or both spectral information retrieval and geometric correction may not match precisely between sensors, resulting in the difference between time steps being driven by differences between sensors rather than real differences in reflectance on the ground. Fusing data from sensors that are even more different, such as with different spatial resolutions and projections, is even more challenging. On the other hand, a machine learning approach could make use of data from different sensors easier, as the data they provide would be treated as separate variables, that may potentially help to predict the location of selective logging features.

6 Conclusion

1. 43% of all known treefall gaps were discernible with confidence from the surrounding forest in Sentinel-2 MSI image time series, but none could be discerned with confidence from Landsat 7 ETM+ or Landsat 8 OLI imagery; skid trails were not discernible in any of the imagery, whereas logging roads and log decks were discernible in all of the imagery. It was not possible to automate detection of treefall gaps using Sentinel-2 MSI imagery because of the short time series length and frequent cloud cover.

2. NDMI was found to be the most sensitive index to newly created treefall gaps (change magnitude of -0.15) due to its sensitivity to internal shadowing in forests but low sensitivity to cloud shadows. NDVI was found to be a good indicator of large gaps with soil background. EVI was found to be insensitive to thin cloud cover, but also less sensitive to newly formed treefall gaps (change magnitude of -0.04).

Acknowledgements

I would like to thank Jose Gonzalez de Tanago Menaca and Alvaro Lau Sarmiento for producing and providing the raw data of treefall gap locations in the study sites used in this thesis, a description of the ecological and social background of the study sites, as well as the description of data collection protocols.

Acronyms

ASTER **A**dvanced **S**paceborne **T**hermal **E**mission and Reflection **R**adiometer. 11–13, 18, 19, 25, 31, 38–41

BFAST **B**reaks **F**or **A**dditive **S**eason and **T**rend. 19, 25–28

DBH **D**iameter at **B**reast **H**eight. 16, 19, 21, 22, 33

ESA **E**uropean **S**pace **A**gency. 11

ESPA Earth Resources Observation and Science (**E**ROS) Center **S**cience **P**rocessing **A**rchitecture. 11, 18

ETM+ **E**nhanced **T**hematic **M**apper **Plus**. 11, 13, 14, 16, 18, 25, 28, 37, 38, 40, 41, 43, 45

EVI **E**nhaced **V**egetation **I**ndex. 12, 13, 24, 31, 36–38, 45

GiB **G**ib**ib**ytes. 36, 37

GPS **G**lobal **P**ositioning **S**ystem. 14

MSAVI **M**odified **S**oil **A**djusted **V**egetation **I**ndex. 12, 13, 18, 24, 31, 37, 38

MSI **M**ulti-**s**pectral **I**mager. 11, 13, 16, 19, 21–23, 25, 26, 30, 33, 36–42, 45

NA **N**ot **A**vailable. 18

NBR **N**ormalised **B**urn **R**atio. 12, 13, 18, 24, 29, 31, 36–38, 41

NDMI **N**ormalised **D**ifference **M**oisture **I**ndex. 13, 18, 21, 24–26, 28, 29, 31, 33–38, 45

NDVI **N**ormalised **D**ifference **V**egetation **I**ndex. 12, 18, 21, 24, 25, 27–29, 31, 33–39, 41, 45

NIR **N**ear **I**nfra**r**ed. 11–13, 29, 31, 33, 38

OLI **O**perational **L**and **I**mager. 11, 13, 14, 16, 18, 25–27, 36–39, 43, 45

RAM **R**andom **A**ccess **M**emory. 37

REDD+ **R**educing **E**missions from **D**eforestation and forest **D**egradation. 8

RIL **R**educed-**I**mpact **L**ogging. 7, 14, 21, 25, 35, 40, 41

SAVI **S**oil **A**djusted **V**egetation **I**ndex. 12, 13

SWIR **S**hort**w**ave **I**nfra**r**ed. 11–13, 18, 29, 31, 38, 40

USGS **U**.**S**. **G**eological **S**urvey. 11, 12

UTM **U**niversal **T**ransverse **M**ercator. 11, 19

WUR **W**ageningen **U**niversity & **R**esearch. 14

Bibliography

Asner, G. P., Broadbent, E. N., Oliveira, P. J. C., Keller, M., Knapp, D. E., and Silva, J. N. M. (2006). Condition and fate of logged forests in the Brazilian Amazon. *Proceedings of the National Academy of Sciences*, 103(34):12947–12950.

Asner, G. P., Keller, M., Pereira, Rodrigo, J., Zweede, J. C., and Silva, J. N. M. (2004). Canopy Damage and Recovery After Selective Logging in Amazonia: Field and Satellite Studies. *Ecological Applications*, 14(sp4):280–298.

Asner, G. P., Keller, M., Pereira, R., and Zweede, J. C. (2002). Remote sensing of selective logging in Amazonia. *Remote Sensing of Environment*, 80(3):483–496.

Asner, G. P., Knapp, D. E., Broadbent, E. N., Oliveira, P. J. C., Keller, M., and Silva, J. N. (2005). Selective Logging in the Brazilian Amazon. *Science*, 310(5747):480–482.

Bacour, C., Baret, F., Béal, D., Weiss, M., and Pavageau, K. (2006). Neural network estimation of LAI, fAPAR, fCover and LAI×Cab, from top of canopy MERIS reflectance data: Principles and validation. *Remote Sensing of Environment*, 105(4):313–325.

Broadbent, E. N., Zarin, D. J., Asner, G. P., Peña-Claros, M., Cooper, A., and Littell, R. (2006). Recovery of forest structure and spectral properties after selective logging in lowland Bolivia. *Ecological Applications*, 16(3):1148–1163.

Cibula, W. G., Zetka, E. F., and Rickman, D. L. (1992). Response of thematic mapper bands to plant water stress. *International Journal of Remote Sensing*, 13(10):1869–1880.

Dutrieux, L. and DeVries, B. (2014). bfastSpatial: Set of utilities and wrappers to perform change detection on satellite image time-series. Technical report, Zenodo. DOI: 10.5281/zenodo.49693.

Fragal, E. H., Silva, T. S. F., Novo, E. M. L. d. M., Fragal, E. H., Silva, T. S. F., and Novo, E. M. L. d. M. (2016). Reconstructing historical forest cover change in the Lower Amazon floodplains using the LandTrendr algorithm. *Acta Amazonica*, 46(1):13–24.

Frolking, S., Palace, M. W., Clark, D. B., Chambers, J. Q., Shugart, H. H., and Hurtt, G. C. (2009). Forest disturbance and recovery: A general review in the context of spaceborne remote sensing of impacts on aboveground biomass and canopy structure. *Journal of Geophysical Research: Biogeosciences*, 114(G2):G00E02.

Gonzalez de Tanago Menaca, J., Lau, A., Bartholomeusm, H., Herold, M., Avitabile, V., Raumonen, P., Martius, C., Goodman, R., Disney, M., Manuri, S., Burt, A., and Calders, K. (2017). Estimation of above-ground biomass of large tropical trees with Terrestrial LiDAR. *Methods in Ecology and Evolution*. Accepted Author Manuscript.

Grecchi, R. C., Beuchle, R., Shimabukuro, Y. E., Aragão, L. E. O. C., Arai, E., Simonetti, D., and Achard, F. (2017). An integrated remote sensing and GIS approach for monitoring areas affected by selective logging: A case study in northern Mato Grosso, Brazilian Amazon. *International Journal of Applied Earth Observation and Geoinformation*, 61:70–80.

Haboudane, D., Miller, J. R., Tremblay, N., Zarco-Tejada, P. J., and Dextraze, L. (2002). Integrated narrow-band vegetation indices for prediction of crop chlorophyll content for application to precision agriculture. *Remote Sensing of Environment*, 81(2):416–426.

Hamunyela, E., Verbesselt, J., and Herold, M. (2016). Using spatial context to improve early detection of deforestation from Landsat time series. *Remote Sensing of Environment*, 172(Supplement C):126–138.

Herault, B., Ouallet, J., Blanc, L., Wagner, F., and Baraloto, C. (2010). Growth responses of neotropical trees to logging gaps. *Journal of Applied Ecology*, 47(4):821–831.

Huete, A., Justice, C., and Van Leeuwen, W. (1999). MODIS vegetation index (MOD13): algorithm theoretical basis document. Version 3.

Jackson, S. M., Fredericksen, T. S., and Malcolm, J. R. (2002). Area disturbed and residual stand damage following logging in a Bolivian tropical forest. *Forest ecology and management*, 166(1):271–283.

Keller, M., Asner, G. P., Silva, N., and Palace, M. (2004). 4. Sustainability of Selective Logging of Upland Forests in the Brazilian Amazon Carbon Budgets and Remote Sensing as Tools for Evaluating Logging Effects. In *Working Forests in the Neotropics Conservation through Sustainable Management?* De Gruyter, Berlin, Boston. DOI: 10.7312/zari12906-006.

Kennedy, R. E., Yang, Z., and Cohen, W. B. (2010). Detecting trends in forest disturbance and recovery using yearly Landsat time series: 1. LandTrendr — Temporal segmentation algorithms. *Remote Sensing of Environment*, 114(12):2897–2910.

Key, C. H., Benson, N., Ohlen, D., Howard, S. M., and Zhu, Z. (2002). The normalized burn ratio and relationships to burn severity: ecology, remote sensing and implementation. In *Ninth biennial remote sensing applications conference, Apr 8–12, San Diego, CA*.

Kleinschroth, F., Healey, J. R., Sist, P., Mortier, F., and Gourlet-Fleury, S. (2016). How persistent are the impacts of logging roads on Central African forest vegetation? *Journal of Applied Ecology*, 53(4):1127–1137.

Meyer, D., Siemonsma, D., Brooks, B., and Johnson, L. (2015). Advanced Spaceborne Thermal Emission and Reflection Radiometer Level 1 Precision Terrain Corrected Registered At-Sensor Radiance (AST_L1T) Product, Algorithm Theoretical Basis Document. Technical report, US Geological Survey.

Mueller-Wilm, U. (2016). Sen2cor Configuration and User Manual. Ref. S2-PDGS-MPC-L2A-SUM-V2.3.

NASA LP DAAC (2006). ASTER On-Demand L2 Surface Reflectance VNIR and SWIR Crosstalk-Corrected. DOI: 10.5067/ASTER/AST_07XT.003.

Pinard, M. and Cropper, W. (2000). Simulated effects of logging on carbon storage in dipterocarp forest. *Journal of Applied Ecology*, 37(2):267–283.

Piponiot, C., Sist, P., Mazzei, L., Peña-Claros, M., Putz, F. E., Rutishauser, E., Shenkin, A., Ascarrunz, N., Azevedo, C. P. d., Baraloto, C., França, M., Guedes, M., Coronado, E. N. H., d'Oliveira, M. V., Ruschel, A. R., Silva, K. E. d., Sotta, E. D., Souza, C. R. d., Vidal, E., West, T. A.,

and Hérault, B. (2016). Carbon recovery dynamics following disturbance by selective logging in Amazonian forests. *eLife*, 5:e21394.

Qi, J., Chehbouni, A., Huete, A. R., Kerr, Y. H., and Sorooshian, S. (1994). A modified soil adjusted vegetation index. *Remote Sensing of Environment*, 48(2):119–126.

Qiu, S., He, B., Zhu, Z., Liao, Z., and Quan, X. (2017). Improving Fmask cloud and cloud shadow detection in mountainous area for Landsats 4–8 images. *Remote Sensing of Environment*, 199(Supplement C):107–119.

Read, J. M. (2003). Spatial analyses of logging impacts in Amazonia using remotely sensed data. *Photogrammetric Engineering & Remote Sensing*, 69(3):275–282.

Rutishauser, E., Hérault, B., Baraloto, C., Blanc, L., Descroix, L., Sotta, E. D., Ferreira, J., Kanashiro, M., Mazzei, L., d'Oliveira, M. V. N., de Oliveira, L. C., Peña-Claros, M., Putz, F. E., Ruschel, A. R., Rodney, K., Roopsind, A., Shenkin, A., da Silva, K. E., de Souza, C. R., Toledo, M., Vidal, E., West, T. A. P., Wortel, V., and Sist, P. (2015). Rapid tree carbon stock recovery in managed Amazonian forests. *Current Biology*, 25(20):2738.

Rutishauser, E., Hérault, B., Petronelli, P., and Sist, P. (2016). Tree Height Reduction After Selective Logging in a Tropical Forest. *Biotropica*, 48(3):285–289.

Schneibel, A., Stellmes, M., Röder, A., Frantz, D., Kowalski, B., Haß, E., and Hill, J. (2017). Assessment of spatio-temporal changes of smallholder cultivation patterns in the Angolan Miombo belt using segmentation of Landsat time series. *Remote Sensing of Environment*, 195:118–129.

Scullion, J. J., Vogt, K. A., Sienkiewicz, A., Gmur, S. J., and Trujillo, C. (2014). Assessing the influence of land-cover change and conflicting land-use authorizations on ecosystem conversion on the forest frontier of Madre de Dios, Peru. *Biological Conservation*, 171(Supplement C):247–258.

Shimizu, K., Ponce-Hernandez, R., Ahmed, O. S., Ota, T., Win, Z. C., Mizoue, N., and Yoshida, S. (2017). Using Landsat time series imagery to detect forest disturbance in selectively logged tropical forests in Myanmar. *Canadian Journal of Forest Research*, 47(3):289–296.

Souza, C. M., Roberts, D. A., and Cochrane, M. A. (2005). Combining spectral and spatial information to map canopy damage from selective logging and forest fires. *Remote Sensing of Environment*, 98(2):329–343.

SUHET (2015). Sentinel-2 user handbook. Revision 2.

Tucker, C. J., Elgin, J. H., McMurtrey, J. E., and Fan, C. J. (1979). Monitoring corn and soybean crop development with hand-held radiometer spectral data. *Remote Sensing of Environment*, 8(3):237–248.

U.S. Geological Survey (2017a). Product guide: Landsat 4-7 Surface Reflectance (LEDAPS) product. Version 7.9.

U.S. Geological Survey (2017b). Product guide: Landsat 8 Surface Reflectance Code (LaSRC) product. Version 4.0.

U.S. Geological Survey (2017c). Product guide: Landsat surface reflectance-derived spectral indices. Version 3.5.

Verbesselt, J., Hyndman, R., Newnham, G., and Culvenor, D. (2010). Detecting trend and seasonal changes in satellite image time series. *Remote Sensing of Environment*, 114(1):106–115.

West, T. A. P., Vidal, E., and Putz, F. E. (2014). Forest biomass recovery after conventional and reduced-impact logging in Amazonian Brazil. *Forest Ecology and Management*, 314:59–63.

Zhu, Z., Wang, S., and Woodcock, C. E. (2015). Improvement and expansion of the Fmask algorithm: cloud, cloud shadow, and snow detection for Landsats 4–7, 8, and Sentinel 2 images. *Remote Sensing of Environment*, 159:269–277.

Zhu, Z. and Woodcock, C. E. (2012). Object-based cloud and cloud shadow detection in Landsat imagery. *Remote Sensing of Environment*, 118(Supplement C):83–94.